

**Synthesis of Antibacterial/ Anti biofilm
Nanoparticles and ~~t~~Their Coating on
Artificial Teeth to Inhibit Oral Diseases**

Michal Eshed

Department of Chemistry

Ph.D. Thesis

Submitted to the Senate of Bar-Ilan University

Ramat-Gan, Israel

October, 2013

This work was carried out ~~by~~under the supervision of

Prof. Aharon Gedanken

from the Department of Chemistry

Bar-Ilan University, Ramat-Gan, Israel

*This dissertation is dedicated to my family who always wanted
me to go ~~by~~in the way of knowledge.*

*Thank you for ~~they~~your friendship, ~~for~~the tremendous love and
the support you have given me, and for always believing in me.*

Bar-IanUniversity



NAME OF STUDENT: Michal Eshed

DEGREE AWARDED: Doctor of Philosophy in Chemistry

ACADEMIC UNIT: Department of Chemistry

TITLE OF THESIS: Synthesis of antibacterial/ anti biofilm nanoparticles and their coating on artificial teeth in order to inhibit oral diseases.

This is to certify that the thesis entitled "**Synthesis of Antibacterial/ Anti biofilm Nanoparticles and Their Coating on Artificial Teeth to Inhibit Oral Diseases**" submitted by Michal Eshed to Bar-Ilan University, Israel for the award of the degree of Doctor of Philosophy is a bona fide record of research work carried out by her under my supervision. The content of this thesis, in full or in part, has not been submitted to any other research organization for the award of a degree or a diploma.

Signature of supervisor

Prof. Aharon Gedanken

Date: October 2013.

Acknowledgment

First and foremost I would like to extend my heartfelt gratitude to my supervisor Prof. Aharon Gedanken. I am exceedingly thankful to him for his valuable and inspiring guidance, support, encouragement, understanding, advice and suggestions, through out the period of my research programme. I would like to thank him for his patience in guiding me through my mistakes and forhis constant encouragement that helped in shaping my scientific perception. His enthusiasm, hard work, discipline, and dedication to science and research have been a source of great inspiration and motivation tofor me.

I am also indebted to Dr. Ehud Banin, Faculty of Life Sciences, for his great collaboration, patience and understanding, during my work and also during ~~with~~ the ~~writing-compilation~~ of the related papers.

Special thanks to Dr. Jonathan Lellouche, who shared with me his expertise in the field of microbiology. I appreciate his collaboration, trulydedication to this project, and his continualed support, guidance, and professional advices all the way. I will always be grateful to him for teaching me ~~so much~~ with patience and understanding. I consider it a privilege to learn and work with him.

I would like to express my appreciation and thanks to Dr. Shlomo Matalon, Prof. Nina Perkas, Prof. Yuri Koltypin and Mrs. Galina Amirian for their expert advice and ~~for their~~ kind help.

Thanks to Dr. Anat Lipovsky for her support, help and efficient advices in the field of microbiology.

Thanks to Dr. Yosi Taljoseff for helping in my HR-SEM measurements, and to the administrative staffs of the Department of Chemistry, and the Bar-Ilan Nanotechnology and Advanced Materials Center.

I cannot sufficiently express my thanks to my colleagues in Prof. Gedanken's laboratory group for the interesting discussions, ~~their~~ friendship and for their kind help.

Above all, I wish to express my endless gratitude to my parents, Liora and Danny Eshed, and my brother Eyal, for their constant encouragement and heartfelt support, for all their love, and encouragement throughout the years. Without you, I never could have made it through this. Thank you!

Formatted: Indent: First line: 1.27 cm

I would also like to thank my late grandmother, Sara Kirsholtz, who has always done everything to support my education and who would have liked to have seen its completion.

Table of Contents

Acknowledgments

List of Contents

List of Figures

List of Tables

Abbreviations

Abstract

1. Introduction.....	<u>1</u>
1.1 Nanomaterials and Nanotechnology [1]	<u>1</u>
1.2 Nanosynthesis	<u>2</u>
1.3 Classifications of nanomaterials	<u>3</u>
1.4 Bacteria	<u>4</u>
1.5 Biofilm	<u>5</u>
1.5.1 Dental plaque as a biofilm [9].....	<u>6</u>
1.6 Mechanisms of biofilm resistance	<u>8</u>
1.7 Plaque biofilms and disease	<u>10</u>
1.8 <i>Streptococcus mutans</i> (<i>S. mutans</i>) - gram-positive organism.....	<u>12</u>
1.9 Antimicrobial and antibiofilm coatings	<u>15</u>
1.9.1 Biocide-release: matrix impregnated coatings.....	<u>15</u>
1.9.2 Microbe-repelling coatings	<u>16</u>
1.9.3 Contact-active coatings: surface-modified coatings	<u>17</u>
1.10 The use of nanoparticles as antimicrobial materials	<u>18</u>
1.10.1 The <u>u</u> se of <u>n</u> Nanoparticles to <u>c</u> ontrol <u>o</u> ral <u>b</u> Biofilm <u>f</u> ormation [57]	<u>20</u>
1.11 Biochemical actions of fluoride on oral biofilm [94]	<u>23</u>
1.11.1 Biochemical actions of fluoride on microorganisms	<u>24</u>
1.12 Sonochemical synthesis	<u>25</u>
1.12.1 Introduction.....	<u>25</u>
1.12.2. Sound, Ultrasound, and Cavitation	<u>26</u>
1.12.3 The Sonochemical Hot-Spot.....	<u>28</u>

1.12.4 Sonochemistry in nanomaterial synthesis.....	2929
2. Research Objectives.....	3232
2.1 Research importance.....	3232
2.2 Research goals.....	3232
2.2.1 Major goals.....	3232
2.2.2 Minor goals.....	3232
2.3 Novelty of the Research.....	3333
3- Experimental System.....	3434
3.1 Teeth used in this research.....	3535
3.2 <u>Preparation Synthesis</u> of NP coated teeth.....	3535
3.2.1 ZnO and CuO NPs synthesis and coating procedure.....	3636
3.2.2 Zn-CuO NPs synthesis and coating procedure.....	3636
3.2.3 MgF ₂ synthesis and coating procedure.....	3737
3.3 Characterization methods.....	3737
3.3.1 Transmission Electron Microscopy (TEM).....	3737
3.3.2 Scanning Electron Microscopy (SEM).....	3838
3.3.3 Elemental Analysis.....	3939
3.3.4 Inductively coupled plasma (ICP).....	3939
3.3.5 Rutherford Backscattering Spectrometry (RBS).....	3939
3.3.6 Electron <u>S</u> pin <u>R</u> esonance spectroscopy (ESR).....	3939
3.3.7 Confocal Microscopy.....	4040
3.3.8 Atomic Force Microscope (AFM).....	4040
3.3.9 Zeta potential.....	4141
3.3. 10 Focused Ion Beam (FIB).....	4141
4- Integration of the Research Articles.....	4242
4.1 List of articles:.....	4242
4.2 Integration of the research articles.....	4242
4.3 List of the articles and their abstracts.....	4444
4.3.1 Article 1.....	4444
4.3.2 Article 2.....	4545
4.3. 3 Article 3.....	4646
5- Discussion.....	4747
5.1 Article 1.....	4747
5.2 Article 2.....	5151
5.3 Article 3.....	5656
5.4 Conclusions.....	6060
6 - References.....	6161

List of figures	Pages
Figure 1.1. Structure and constituents of a typical bacterial cell	4
Figure 1.2. Gram-positive and -negative cell wall structure	5
Figure 1.3. Five stages of biofilm development	8
Figure 1.4. Biofilms resistance mechanisms	10
Figure 1.5. Progression of untreated periodontal disease	11
Figure 1.6. Bacterial accretion and multigeneric coaggregation during the formation of dental plaque	13
Figure 1.7. Schematic representation of describes in details the attachment of <i>S. mutans</i> to tooth surfaces	15
Figure 1.8. The functioning of the biocide release coating and the antimicrobial activity of the coating	17
Figure 1.9. The functioning of the hydrogel coating without and the antimicrobial activity of the coating	18
Figure 1.10. The functioning of the surface-modified coating and (B) the antimicrobial activity of the coating	19
Figure 1.11. Bubble growth and implosion	29
Figure 3.1. Artificial acryl teeth	35
Figure 3.2. Experimental setup for sonochemical reaction	36
Figure 5.1. Schematic illustration of the antibacterial mechanism of CuO NPs and the relative cellular structure	51
Figure 5.2. Defense mechanism against damage by ROS. Superoxide dismutase (SOD) plus catalase or glutathione peroxidase (GPx)	52
Figure 5.3. Mechanism of lipid peroxidation	58
Figure 5.4. Illustration comparing bacteria-the surface interactions of bacteria with nanorough surfaces and conventional nanosmooth surfaces	61

List of tables	Pages
Table 1.1. Summary of select <u>ed</u> studies concerning <u>on</u> the antimicrobial effects of nanoparticles-	21
Table 5.1. Various components of saliva and their functions-	59

Abbreviations

A

AEP- acquired enamel pellicle

AFM- atomic force microscope

C

CuO- cupric oxide

E

E. coli- *Escherichia coli*

EDS- energy dispersive X-ray spectroscopy

EPS- extracellular polymeric substances

ESR- electron spin resonance

F

FE-field emission

FIB- focused ion beam

G

GBP- glucan-binding protein

GCF- gingival crevicular fluid

GPx- glutathione peroxidase

Gtfs- glucosyltransferases

H

HA- hydroxyapatite

HF- hydrofluoric acid

HR-SEM- high resolution scanning electron microscopy

I

ICP- inductively coupled plasma

M

MDR- multidrugresistance

MEMS-micro-electromechanical systems

N

nm- nanometer

NP/NPs- nanoparticle/nanoparticles

O

OMP- outer membrane proteins

R

RBS-Rutherford backscattering spectrometry

ROS- reactive oxygen species

S

SEM- scanning electron microscopy

S. mutans- *Streptococcus mutans*

SOD- superoxide dismutase

T

TCS-two-component signal

TEM-transmission electron microscopy

TTIP-tetra-isopropoxide

Z

ZnO- zinc oxide

Abstract

Nanotechnology ~~is an enabling technology that~~ deals with nanometer size objects. It is expected that nanotechnology will be developed at several levels: materials, devices, and systems. The nanoparticles (NPs) level is the most advanced at present, both in scientific knowledge and in commercial applications. A decade ago, NPs were studied because of their size-dependent physical and chemical properties. Now, they have entered a period of commercial exploration.

The need for novel antibiotics comes from the relatively high incidence of bacterial infection and the growing resistance of bacteria to conventional antibiotics. Biofilm formation is ultimately a defense mechanism for the bacterial community. There are various differences between free-living (i.e. planktonic) and biofilm-bound bacteria, most notably there is a noticeable decrease in susceptibility to antimicrobial agents and harsh environmental conditions in biofilm-protected bacteria. As a result, infections caused by bacterial biofilms are persistent and much more difficult to eradicate than their planktonic counterparts. Biofilms are also a major cause of infections associated with medical implants. Consequently, new methods for reducing bacteria activity are ~~badly~~ needed. Nanotechnology, the use of materials with dimensions on the atomic or molecular scale, has become increasingly utilized for medical applications and is of great interest as an approach to killing or reducing the activity of microorganisms. Nanomaterials possess high antibacterial properties as particle size is reduced into the nanometer regime (due to the increased surface to volume ratio of a given mass of particles), the physical structure of a nanoparticle itself and the way in which it interacts and penetrates into bacteria appears to also provide unique bactericidal mechanisms. In this regard, inorganic NPs in general and metal oxide NPs in particular, as antimicrobial agents, can fulfill the need of a new class of biocidal formulations.

The aim of this work was firstly to use the novel ultrasonic synthetic techniques to fabricate metal oxide and metal fluoride NPs and to coat artificial teeth for antimicrobial and anti biofilm applications. We have demonstrated the antimicrobial activity of these NPs against common oral bacteria, *Streptococcus mutans* (*S. mutans*) which plays an important role in the development of dental caries.

We have prepared ZnO, CuO, Zn-doped CuO composite, ($\text{Cu}_{0.88}\text{Zn}_{0.12}\text{O}$, noted Zn-CuO) and MgF_2 NPs (as bactericidal NPs), together with the optimization of process parameters (e.g. selection of the precursors, temperature, reaction time, reaction atmospheres and; concentration of reactants ~~etc.~~) in order to obtain the desired nanostructures with suitable conditions for biological applications.

All the NPs that were investigated in this study have impressive anti biofilm activity with a varied level of efficiency. We demonstrated that the antibiofilm activity of MgF_2 NPs may be due to surface modifications caused during the coating process such as, high roughness and hydrophobicity of tooth surface. Only Zn-doped CuO NPs have shown some antibacterial activity against *S. mutans* bacteria which finally lead to enhancement in its antibiofilm activity as well. A possible ~~potential~~ mechanism of action is also suggested for these NPs. The other coated NPs (MgF_2 , ZnO and CuO) have inhibited the formation of biofilm of *S. mutans* on the artificial teeth but didn't kill the bacteria. Transmission electron microscopic technique indicated that the NPs attach to and penetrate into the cells and consequently generate intracellular reactive oxygen species (ROS) which enhance lipid peroxidation and cause cell death. Our results further highlight the improved efficacy of the Zn-CuO nano-composites over CuO and ZnO NPs and the role of ROS in their mechanism of action.

Taken together, these results highlight the future potential of developing these NPs to inhibit biofilm formation in the context of the oral niche.

1. Introduction

1.1 Nanomaterials and Nanotechnology

Nanoparticles are of great scientific interest as they ~~are~~ effectively a bridge [the gap](#) between bulk materials and atomic or molecular structures.

Nanoparticles exhibit a number of special properties relative to bulk material. For example, the bending of bulk copper (wire, ribbon, etc.) occurs with movement of copper atoms/clusters at about the 50 nm scale. Copper nanoparticles smaller than 50 nm are considered super hard materials that do not exhibit the same malleability and ductility as bulk copper. The change in properties is not always desirable. Ferroelectric materials smaller than 10 nm can switch their magnetisation direction using room temperature thermal energy, thus making them useless for memory storage [1].

Nanotechnology deals with small structures or small-sized materials. Typical dimensions span from sub nanometer to several hundred nanometers. A nanometer (nm) is one billionth of a meter, or 10^{-9} m. One nanometer is approximately a length equivalent to 10 hydrogen or 5 silicon atoms aligned in a straight line. Small features permit [greater-more](#) functionality in a given space, but nanotechnology is not only a simple continuation of miniaturization from microm~~e~~-meter scale down to nanometer scale. A bulk material should have constant physical properties regardless of its size. Size-dependent properties are observed such as quantum confinement in semiconductor particles, surface plasmon resonance in some metal particles and super paramagnetism in magnetic materials, crystals in the nanometer scale have a low melting point (the difference can be as large as 1000_°C) and reduced lattice constants. The interesting and sometimes unexpected properties of nanoparticles are partly due to the aspects of the surface of the material dominating the properties in lieu of the bulk properties. Since the number of surface atoms or ions becomes a significant fraction of the total number of atoms or ions, and the surface energy plays a significant role in the thermal stability. Crystal structures stable at elevated temperatures are stable at much lower temperatures in nanometer sizes, so ferroelectrics and ferromagnetics may lose their ferroelectricity and ferromagnetism when the materials are shrunk to the nanometer scale. Bulk semiconductors become insulators when the characteristic dimension is sufficiently small (a couple of nanometers). Although bulk gold does not exhibit catalytic properties, Au nanocrystal

has been demonstrated to be an excellent low temperature catalyst. Currently there are many different opinions about what exactly is nanotechnology. For example, some people consider the study of microstructures of materials using electron microscopy and the growth and characterization of thin films as nanotechnology. Other people consider a bottom-up approach in materials synthesis and fabrication, such as self assembly or biomineralization to form hierarchical structures like abalone shells, to be nanotechnology. Drug delivery, e.g. inserting drugs inside carbon nanotubes, is regarded as nanotechnology. Micro-electromechanical systems (MEMS) and lab-on-a-chip are also considered nanotechnology. More futuristic or science fiction-like opinions are that nanotechnology means something very ambitious and startlingly new, such as miniature submarines in the bloodstream, smart self-replication nanorobots monitoring our body, space elevators made of nanotubes, and the colonization of space. There are many other definitions that people working in nanotechnology use to define the field. These definitions are true to certain specific research fields, but none of them covers the full spectrum of nanotechnology. The many diverse definitions of nanotechnology reflect the fact that nanotechnology covers a broad spectrum of research and requires true interdisciplinary and multidisciplinary efforts. In general, nanotechnology can be understood as a technology of design, fabrication and application of nanostructures and nanomaterials. In order to explore novel physical properties and phenomena and realize potential applications of nanostructures and nanomaterials, the ability to fabricate and process nanomaterials and nanostructures is the first corner stone in nanotechnology. Nanostructured materials are those with at least one dimension falling in the nanometer scale, and include nanoparticles (including quantum dots, when exhibiting quantum effects), nanorods and nanowires, thin films, and bulk materials made of nanoscale building blocks or consisting of nanoscale structures [1].

1.2 Nanosynthesis

There are a few widely known methods to produce nanomaterials. The list includes sol-gel, aerogels, aerosol spray pyrolysis, inverse micelle methods, reactive evaporation of metals, zintl salts, inert gas condensation, mechanical alloying or high-energy ball milling, plasma synthesis, and electrodeposition etc. The pioneering synthetic approaches have been invaluable in establishing the new field of scientific

endeavor: nanostructured materials. All these processes synthesize nanomaterials to varying degrees of commercially-viable quantities. To date, only the sol-gel [2] synthesis is widely used industrially, since it is easy, economical, can form various homogeneous, bulk, purity nanoproducts at relatively low temperatures.

Sonochemical synthesis is of great interest both from a fundamental scientific point of view and because of its potential for technological advances [3]. Sonochemistry is an additional and comparatively new technique that has been used for the nanosynthesis and modification of inorganic materials. The application of ultrasound in materials science has proved to be an efficient technique in preparation of oxides, metals, alloys, nitrides ~~and polymers, etc.~~ Sonochemical methods also ~~well-known~~ qualify for the ~~task of~~ deposition ~~task~~ (nanocoatings) due to the ability to combine the synthesis of variety of nanomaterials and their simultaneous deposition on various substrates in a single-step operation. The sonochemical method is simple, efficient, and is operated at ambient conditions and can produce uniform coating (that is not possible with other methods). Apart from this, one of the significant advantages is the ability to control the particle size of the product/ nanocoating by varying the concentration of the precursors in the solution. By this method a wide range of substrates are effectively coated [4, 5, 6] with nanosized metals, metal-oxides and magnetic materials.

1.3 Classifications of nanomaterials

Every known substance and every material yet to be discovered will yield a new set of properties, depending on size. Optical properties, magnetic properties, melting points, specific heats, and crystal morphologies can all be influenced because nanomaterials serve as a bridge between the molecular and condensed phases. ~~The thousands of~~ Many substances that are solids under normal temperatures and pressures can be subdivided into metals, ceramics, semiconductors, composites, and polymers. These can be further divided into biomaterials, catalytic materials, coatings, glass, magnetic and electronic materials [7]. All of these solid substances, with their widely variable properties, take on another subset of new properties when produced in nanoform. The possibilities are endless. Chemistry and chemists have a leadership role if this new field is to prosper. The field of nanostructured materials has evolved; many names and labels have been used. Their definitions [8] are briefly given below.

1. Nanoparticle: A solid particle in the 1-100 nm range that could be noncrystalline, amorphous, an aggregate of crystallites, or a single crystallite.
2. Nanocrystal: A solid particle that is a single crystal in the nanometer size range.
3. Nanostructured or nanoscale or nanophase material: Any solid material that has a nanometer dimension: three dimensions→ particles; two dimensions→ thin film; one dimension→ thin wire.
4. Quantum dots: A particle that exhibits a size quantization effect in at least one dimension.
5. Cluster: A collection of units (atoms or reactive molecules)
6. Colloid: A stable liquid phase containing particles in the 1-1000 nm range.

1.4 Bacteria

The bacteria (*singular*: bacterium) are a group of unicellular microorganisms. Typically a few micrometers in length, bacteria have a wide range of shapes, ranging from spheres to rods and spirals. Bacteria are ubiquitous in every habitat on earth, growing in soil, acidic hot springs, radioactive waste, seawater, and deep in the earth's crust. There are approximately five million (5×10^6) bacteria on earth, forming much of the world's biomass. Bacteria are vital in recycling nutrients, and many important steps in nutrient cycles depend on bacteria, such as the fixation of nitrogen from the atmosphere.

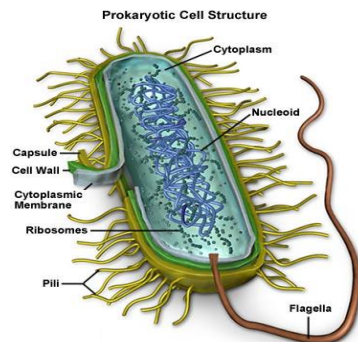


Figure 1.1. Structure and contents of a typical bacterial cell.

The study of bacteria is known as bacteriology, a branch of microbiology. Based on the chemical and physical properties of the bacteria and their cell walls, Gram staining (or Gram's method) is an empirical method that is used for

differentiating bacterial species into two large groups: (Gram-positive and Gram-negative). Gram-positive bacteria are those that are stained dark blue or violet by Gram staining. This is in contrast to gram-negative bacteria, which cannot retain the crystal violet stain, instead taking up the counterstain (safranin or fuchsin) and appearing red or pink. Gram-positive organisms are able to retain the crystal violet stain because of the thick peptidoglycan layer. Gram-negative bacteria are bacteria that do not retain crystal violet dye in the Gram staining protocol. In a Gram stain test, a counterstain (commonly safranin) is added after the crystal violet, coloring all gram-negative bacteria with a red or pink color. The counterstain is used to visualize the otherwise colorless gram-negative bacteria whose much thinner peptidoglycan layer does not retain crystal violet. Compared with to gram-positive bacteria, gram-negative bacteria are more resistant against antibiotics, despite their thinner peptidoglycan layer, because of their additional, relatively impermeable cell wall.

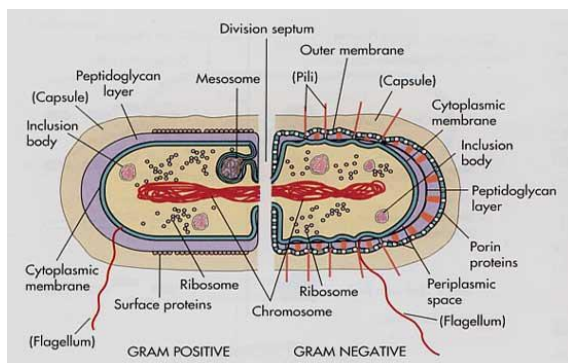


Figure 1.2. Gram-positive and -negative cell wall structure.

1.5 Biofilm

A majority of bacteria in natural and clinical settings are contained in biofilms, which are surface-mounted, integrated communities of cells. Biofilms are highly structured and physically dynamic, with their structure and mechanical properties

defined by extracellular polymeric substances (EPS), which serve as a scaffolding or glue holding the biofilm together.

The life cycle of a biofilm is characterized by attachment of planktonic bacteria to a surface or by migration or division of sessile cells to cover an empty region of the surface, production of EPS to adhere cells irreversibly to the substrate, and then by additional EPS production, cellular motility and reproduction, and phenotypic differentiation to produce a mature, thick and spatially structured biofilm [9].

In EPS production and in many other ways, bacteria in biofilms are phenotypically distinct from their genomically-identical planktonic counterparts. Bacteria in biofilms can be up to 1000 times more resistant to antibiotics, and less conspicuous to the immune system, because antigens are hidden and key ligands are suppressed [10].

1.5.1 Dental plaque as a biofilm

The moment a baby passes through the birth canal and takes its first breath, microbes begin to reside in its mouth [12]. Later, as the teeth erupt, additional bacteria establish colonies on the tooth surfaces. Dental bacterial plaque is a biofilm that adheres tenaciously to tooth surfaces, restorations, and prosthetic appliances [12]. The tooth surface is unique among body surfaces in that it is a nonshedding hard surface, which selectively adsorbs various acidic glycoproteins (mucins) from the saliva, forming what is known as the acquired enamel pellicle (AEP) [13,14]. The AEP is an amorphous membranous layer which varies in thickness from 0.1 to 3 μm , and as it contains a high number of sulfate and carboxyl groups, it further increases the net negative charge of the tooth surfaces [15]. As bacteria also have a net negative charge, there then exists an initial repulsion between the tooth surface and those bacteria in the saliva which approach this surface. This innate defense mechanism breaks down when plaque formation occurs.

Dental plaque is formed via an ordered sequence of events [16,17]. Microcolony formation begins once the surface of the tooth has been covered with attached bacteria. The biofilm grows primarily through cell division of the adherent bacteria, rather than through the attachment of new bacteria. Early colonizing bacteria attach to the acquired pellicle that adsorbs immediately to the tooth surface after cleaning.

These early colonizers grow, modify the environment, and make conditions suitable for colonization by later, more fastidious bacteria, many of which are obligately anaerobic. Attached organisms synthesize exopolymers such as glucans, which form the biofilm matrix that acts as a scaffold for the biofilm, and is biologically active and able to retain molecules within the plaque. Eventually a thick biofilm develops made up of a diverse community of interacting micro-organisms [18], and the composition becomes stable over time (microbial homeostasis). There are distinct stages in plaque formation [19]:

1. Acquired pellicle formation when molecules derived mainly from saliva are adsorbed onto the tooth surface.
2. Reversible adhesion, which involves weak, long- range, physicochemical interactions between the microbial cell surface and the acquired pellicle.
3. Irreversible adhesion, which involves interactions between specific molecules on the microbial cell surface and complementary receptors present in the acquired pellicle. These interactions are stronger and operate at a relatively short distance.
4. Coadhesion, in which secondary colonizers adhere via cell surface adhesions to receptors on already, attached bacteria [20], leading to an increase in microbial diversity within the developing biofilm. Many of the secondary colonizers have fastidious growth requirements.
5. The attached cells multiply, leading to an increase in biomass and synthesis of exopolymers to form the biofilm matrix.

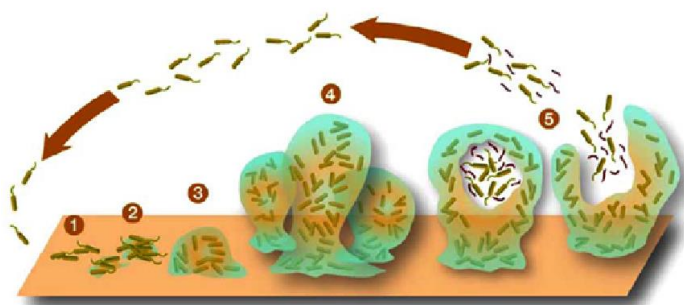


Figure 1.3. Five stages of biofilm development. 1: individual cells populate the surface. 2: EPS is produced and attachment becomes irreversible. 3 and 4: biofilm architecture develops and matures. 5: single cells are released from the biofilm. Figure adopted from [11].

1.6 Mechanisms of biofilm resistance

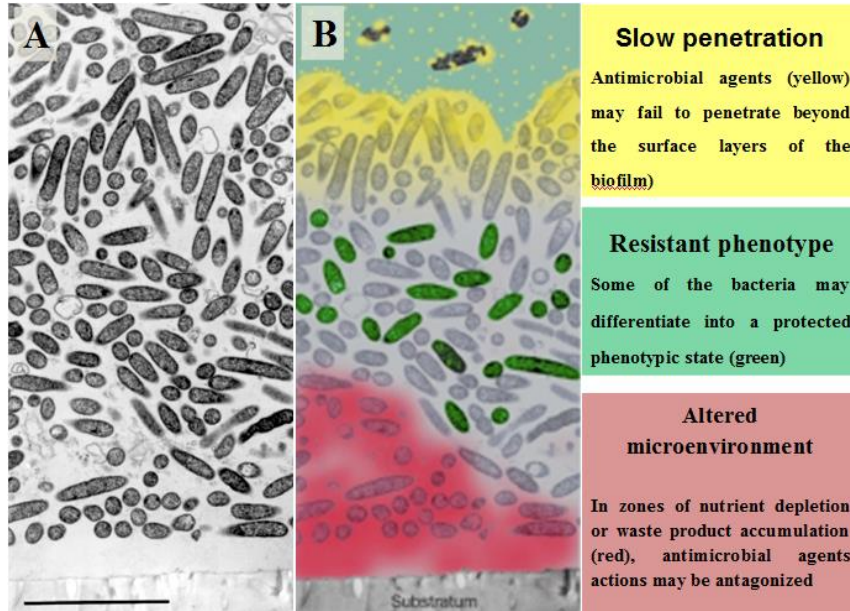
It has been observed that the resistance of biofilms to antibiotics is increased compared ~~with~~ to what is normally seen in planktonic cells. In fact, when cells exist in a biofilm, they can become 100-1000 times more resistant to the effects of antimicrobial agents [21-23]. The development of biocide resistance is not completely understood, but recent studies have suggested various mechanisms that increase biofilm resistance towards antimicrobial agents (**Figure 1.2**). These mechanisms include physical or chemical diffusion barriers to antimicrobial penetration into the biofilm, slow growth of the biofilm owing to nutrient limitation, activation of the general stress response and the emergence of a biofilm-specific phenotype. We will focus here on the main reasons of biofilm resistance properties:

(i) Failure of the antimicrobial to penetrate the biofilm. The production of an exopolysaccharide matrix or glycocalyx. This matrix, among other functions, prevents the access of antimicrobial agents to get to the bacterial cells embedded within the biofilm [23,24]. Thus the cells are protected from the detrimental effects of heat shock, UV and many chemical agents[23] (**Figure 1.2A-B**).

(ii) Heterogeneity, slow growth and the stress response. Biofilms are known to exhibit structural, chemical and biological heterogeneity. The environmental conditions and physiological responses of the bacteria to their local environment are not homogeneous throughout a biofilm. The metabolic activities of the cells, together with diffusional processes, result in concentration gradients of nutrients, signaling compounds and bacterial waste within biofilms. As the bacteria respond to these gradients, they adapt to the local chemical conditions, which can change over time as biofilms develop [25]. For example, inside the biofilm bacteria can encounter a starvation response to a particular nutrient; as a consequence the bacterial cell culture slows its growth. Slow growth of the bacteria has been observed in mature biofilms

and is generally accompanied by physiological changes and increased resistance to antimicrobial agents [26,27] (Figure 1.2C).

(iii) **Special genes regulation and induction of a biofilm phenotype.** A general stress response initiated by growth within a biofilm showed physiological changes that act to protect the cell from various environmental stresses. Thus, the biofilm cells are mediated by the central regulator RpoS (Figure 1.2C). Expression of the RpoS, at high cell density, induces trehalose (an osmoprotectant), catalase, outer membrane proteins (OMP) expression and other molecular pathways [28-30]. Apparently, when cells attach to a surface, they will express a general biofilm phenotype and genes that are activated or repressed in biofilms are different compared with planktonic cells [31]. For example, expression of multidrug (MDR) efflux pumps that can extrude chemically unrelated antimicrobial agents from the cell, such as AcrAB[32] and MexAB-OprM [33] pumps in *E. coli* and *P. aeruginosa* strains, respectively, was shown to be increased in the biofilm mode of growth (Figure 1.2C).



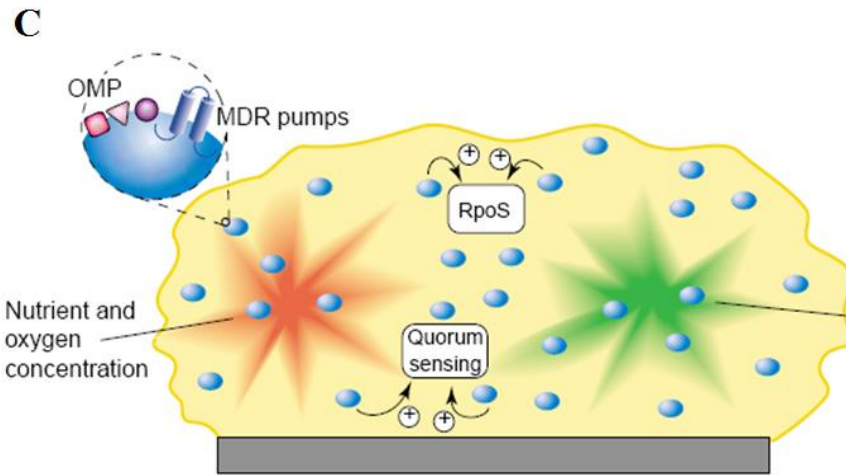


Figure 1.4. Biofilms resistance mechanisms. (A) Electron micrograph of a *P. aeruginosa* biofilm. Bacteria live in multicellular clusters with individual cells in close proximity. Bar=5 μm . (B) and (C) Hypotheses for mechanisms of antimicrobial agent resistance in biofilms. (A-B) adopted from [34] and (C) from [35].

1.7 Plaque biofilms and disease

The disease starts when a bacteria-rich, sticky biofilm called plaque builds up on teeth. Unfortunately, the ability to eradicate the dental biofilm is extremely difficult and simply brushing the teeth is not sufficient. If the plaque remains untreated, it will turn into calculus (tartar) that can only be removed by a dental professional. This plaque buildup eventually results in pockets, a feature caused by gums detaching from the teeth. This allows more plaque and bacteria to reach further into the tissues and cause infection. Infection may lead to more pain (often there is NO pain), swelling of the gums and damage to the gums, tooth roots and bone. The longer the disease goes untreated, the deeper the pocket will grow, and the bone that surrounds the tooth will resorb or melt and create craters, with eventual loosening of the teeth.

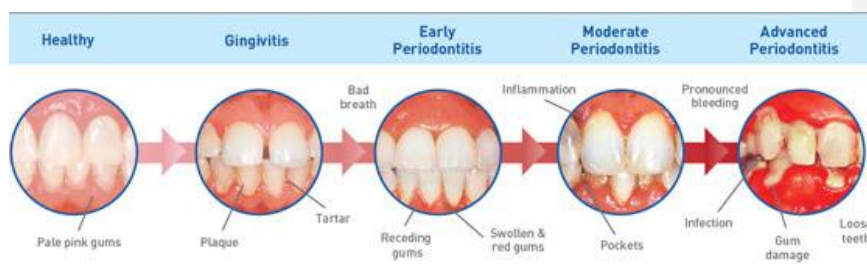


Figure 1.5.Progression of untreated periodontal disease.

Dental caries affect most people in the United States; only 10 percent of late adolescents and young adults are cariesfree [36,37]. Caries continues throughout adulthood, with more than 95 percent of adults experiencing caries on enamel and root surfaces, and it leads to complete loss of teeth in 25 percent of people who then require dentures. Caries prevalence and severity have increased during the past decade in young children, particularly in the primary dentition. Caries, gingivitis and periodontal disease are transmittable infectious diseases that occur because of the accumulation of pathogenic dental plaque [38]. Dental caries is a multifactorial disease that includes the participation of cariogenic and noncariogenic bacteria, salivary components (proteins, enzymes, calcium, phosphate, fluoride) and dietary sources of fermentable carbohydrates (sucrose, glucose) [39,40].

On occasion, microbial homeostasis breaks down in dental plaque, and disease occurs. The microflora from diseased sites is markedly different from that seen in healthy ones [41]. These shifts in microflora occur as a response to changes in environmental conditions that alter the competitiveness of the bacteria, resulting in the selection of previously minor components within the microbial community (ecological plaque hypothesis) [42]. In caries, the regular intake in the diet of fermentable carbohydrates leads to plaque spending more time at a low pH, eventually favouring acidogenic and acid-tolerating species, such as *mutans streptococci*, other acidogenic streptococci, lactobacilli and bifidobacteria, while inhibiting health-associated bacteria that prefer a neutral pH. In contrast, in periodontal disease, excessive plaque accumulation around the gingival margin causes an inflammatory response. The flow of gingival crevicular fluid (GCF) is increased if the host is unable to control this microbial insult, which not only introduces further components of the host response but also molecules such as haemoglobin, haptoglobin and transferrin which select for proteolytic bacteria. These proteolytic bacteria can also degrade host molecules that regulate inflammation, resulting in an exaggerated and inappropriate inflammatory response that can be severe enough to cause by stander damage to host tissues [12].

Clinical studies have shown that caries is associated with increases in the proportions of acidogenic and aciduric (acid-tolerating) bacteria, especially *mutans*

streptococci (such as *S. mutans* and *S. sobrinus*) and lactobacilli, which are capable of demineralizing enamel [43,44]. These bacteria can rapidly metabolize dietary sugars to acid, creating locally a low pH. These organisms grow and metabolize optimally at low pH. Under such conditions they become more competitive, whereas most species associated with enamel health are sensitive to acidic environmental conditions. However, although *mutans streptococci* are strongly implicated with caries, the association is not unique; caries can occur in the apparent absence of these species, while *mutans streptococci* can persist without evidence of detectable demineralization [45,46]. Indeed, in such circumstances, some acidogenic, non-*mutans streptococci* are implicated with disease [47].

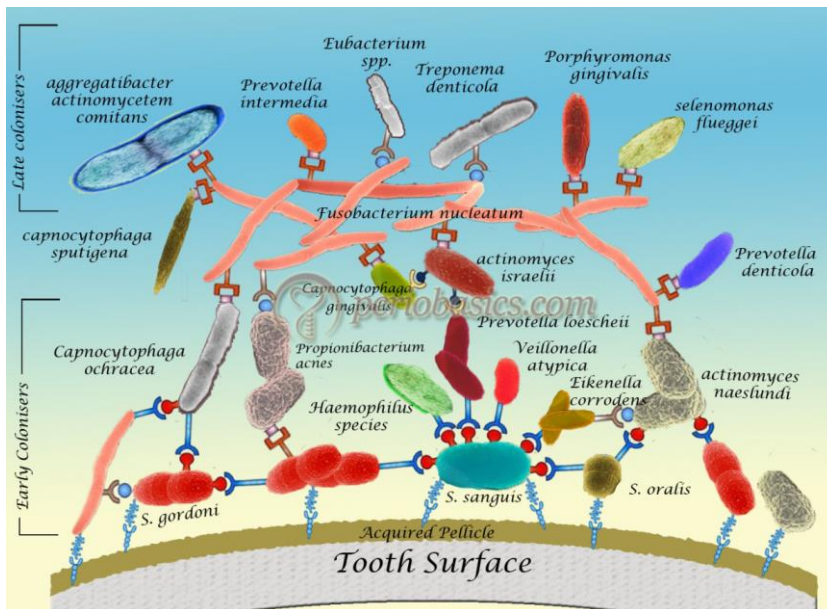
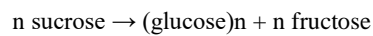


Figure 1.6. Bacterial accretion and multigeneric coaggregation during formation of dental plaque.

1.8 *Streptococcus mutans* (*S. mutans*) - gram-positive organism

The oral microbiota is composed of hundreds of different organisms [48] while *Streptococcus mutans* (*S. mutans*) is regarded as the most potent cariogenic organism and is implicated in all types of dental caries [49], metabolizing sucrose to lactic acid using the enzyme Glucanucrase. *S. mutans*, which grows in biofilms in the oral

niche, ferments sugars and produces acid which lowers the pH and leads to the dissolution of enamel, thus initiating the dental caries process. *S. mutans* is one of a few specialized organisms equipped with receptors that improve adhesion to the surface of teeth. Sucrose is used by *S. mutans* to produce a sticky, extracellular, dextran-based polysaccharide that allows them to cohere, forming plaque. *S. mutans* produces dextran via the enzyme dextransucrase (a hexosyltransferase) using sucrose as a substrate in the following reaction:



However, many other sugars—glucose, fructose, lactose—can be digested by *S. mutans*, but they produce lactic acid as an end-product. It is the combination of plaque and acid that leads to dental decay.

It is also recognized that glucosyltransferases (Gtfs) from *S. mutans* play critical roles in the development of virulent dental plaque. Several groups of oral microorganisms produce Gtfs; these include *Streptococcus sanguinis*, *Streptococcus mutans*, *Streptococcus sobrinus*, *Actinomyces spp*, *Streptococcus salivarius* and *Lactobacillus spp* [50]. Gtfs adsorb to enamel synthesizing glucans in situ, providing sites for avid colonization by microorganisms and an insoluble matrix for plaque. Gtfs also adsorb to surfaces of other oral microorganisms converting them to glucan producers. *S. mutans* expresses 3 genetically distinct Gtfs; each appears to play a different but overlapping role in the formation of virulent plaque. GtfC is adsorbed to enamel within pellicle whereas GtfB binds avidly to bacteria promoting tight cell clustering, and enhancing cohesion of plaque. GtfD forms a soluble, readily metabolizable polysaccharide and acts as a primer for GtfB.

S. mutans organism has developed several mechanisms to maintain its presence in the oral cavity [51] and to withstand drastic environmental changes [52] such as nutrient limitation, oxygen deprivation, antibiotic stress and osmotic shock, which are regulated by the so-called two-component signal transduction system (TCS) pathways [53].

The following scheme describes in details the attachment of *S. mutans* to tooth surfaces:

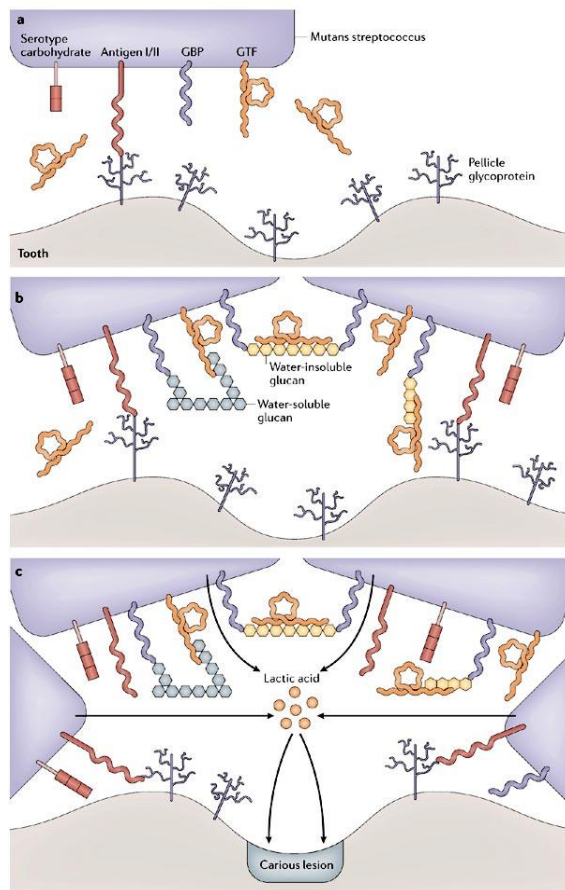


Figure 1.7. Scheme describes in details the attachment of *S. mutans* to tooth surfaces.

a) Initial attachment of *S. mutans* to tooth surfaces. This attachment is thought to be the first event in the formation of dental plaque. The *S. mutans* adhesion (known as antigen I/II) interacts with α -galactosides in the saliva-derived glycoprotein constituents of the tooth pellicle. Other moieties at the surface of mutans streptococci include glucan-binding protein (GBP), serotype carbohydrate and

Gtfs. b) Accumulation of *S. mutans* on tooth surfaces in the presence of sucrose. In the presence of sucrose, Gtfs synthesize extracellular glucans from glucose (after the breakdown of sucrose into glucose and fructose), and this is thought to be the second event in the formation of dental plaque. The *S. mutans* protein GBP is a receptor-like protein that is distinct from Gtfs, and it specifically binds glucans. Gtfs themselves also have a glucan-binding domain and can therefore also function as receptors for glucans. So, *S. mutans* bind pre-formed glucans through GBP and Gtfs, and this gives rise to aggregates of *S. mutans*. c) Acid production by *S. mutans*. The metabolism of various saccharides (including glucose and fructose) by the accumulated bacterial biofilm results in the production and secretion of considerable amounts of the metabolic end-product lactic acid, which can cause demineralization of the tooth structure when present in sufficient amounts in close proximity to the tooth surface. This is thought to be the third event in the formation of dental plaque, and it eventually results in a carious lesion (that is, in dental caries).

1.9 Antimicrobial and antibiofilm coatings

Both socially and economically a great demand exists for antifouling coatings of surfaces. These coatings are for example used in hospitals and biomedical implants to prevent bacterial infections. Three main approaches have been developed to make antimicrobial coatings: biocide-release, microbe-repelling, and contact-active antimicrobial coatings [54].

1.9.1 Biocide-release: matrix impregnated coatings

Basically, a matrix-impregnated coating consists of a polymer matrix that is impregnated with biocides, such as silver ions, halogens and antibiotics. These biocides are then slowly released into the environment, where they kill microbes (Figure 1.6A). Matrix impregnated coatings can be made with a great range of materials. The release of the biocides can be free, controlled or triggered [54]. In the case of free release, biocides burst out of the material immediately, while with controlled release biocides slowly release either by interactions with the material or by degradation of the matrix [54].

Matrix impregnated coating systems are designed to allow for minimal antimicrobial loading and sustained release over a period of weeks [54]. Because the

antimicrobial loading is kept at a minimum, the devices usually do not exhibit observable signs of toxicity[54]. There are a few problems with this type of coating. First, the release of the active component is temporary (**Figure 1.6B**). In the case of implants that are only meant to stay for a short while, the release period of a few weeks is enough. However, a half-life of a few weeks is far too short for more permanent applications, like housecoatings. Also, the substance that leaches out of the coating might be toxic to the environment and the gradually decreasing level of the released compound provides perfect conditions for resistance development.

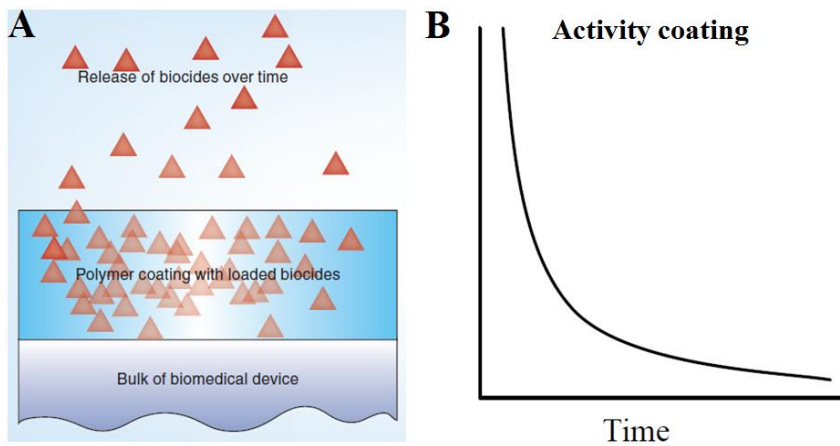


Figure 1.8.(A) The functioning of the biocide release coating and (B) the antimicrobial activity of the coating.

1.9.2 Microbe-repelling coatings

Another approach to obtain an antimicrobial coating is to make a surface microbe repelling. This can be done, for example, by making the surface superhydrophobic which greatly reduces the ability of bacteria to adhere to the surface [55]. Alternatively, the surface can be made extremely hydrophilic by the introduction of hydrogel-forming non-charged coatings, e.g., grafted poly (ethylene glycol)[55]. This can also prevent bacteria from adhering to the surface (**Figure 1.7A**). Hydrogels are three-dimensional, hydrophilic, polymeric networks capable of taking up large amounts of water or biological fluids[55]. The networks are composed of homopolymers or copolymers and are insoluble due to the presence of chemical or physical

cross-links[55]. A common approach for making a hydrogel coating is to physically anchor a longchain hydrophilic polymer in a supporting polymer network that is normally non-swell able in water. One end of the long hydrophilic polymer becomes entwined within the supporting polymer and the free end can become hydrated. The main disadvantage of hydrogels is their poor mechanical properties and toughness after swelling. When an additional antimicrobial agent is incorporated in the hydrogel coating, similar disadvantages to those of the biocide release coatings are observed, especially decreasing activity of the coating over time (**Figure 1.7B**).

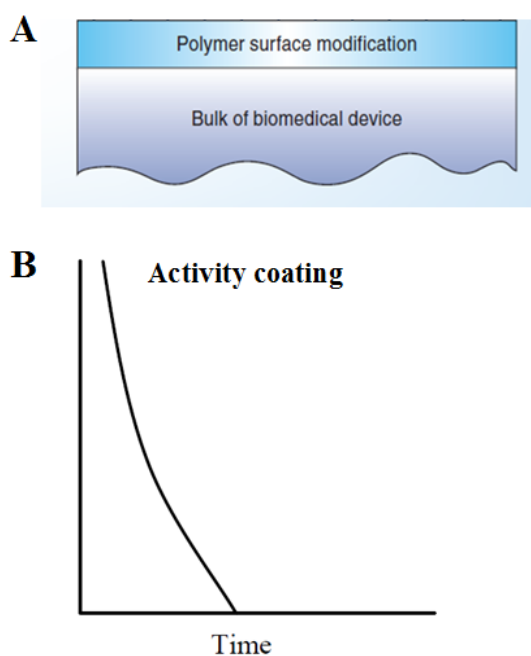


Figure 1.9.(A) The functioning of the hydrogel coating without and (B) the antimicrobial activity of the coating.

1.9.3 Contact-active coatings: surface-modified coatings

A more recent approach was realized by surface modifications that kill microbes on contact without releasing an exhaustible antimicrobial compound. Such systems are based on antimicrobial polymers, e.g., poly (N-alkyl-4-vinylpyridinium salts), in which the antimicrobial compound is a part of the polymer backbone

[54,56]. Covalent attachment can keep a drug present at the surface. The functional groups introduced on the surface of the support, as well as amine, carboxyl or aldehyde groups of the antibiotic, can take part in the formation of stable bonds between the drug and the biomaterial [54,56]. The active agent is bounded by hydrolytically stable linkages, thus enabling prolonged antimicrobial action without significant release of toxic materials (**Figure 1.8A**) [54,56]. Because the amount of available drug is limited and there is no release of drug from the device into the adjacent fluid or tissue, the antimicrobial properties of covalently attached agents are limited [54,56] (**Figure 1.8B**). Another problem of the coating might be that dead bacteria stick to the surface, thereby limiting the available surface-active groups that can kill other bacteria [54,56].

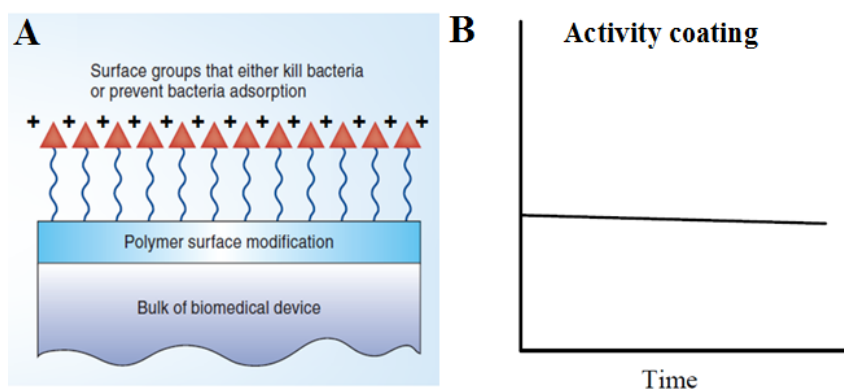


Figure 1.10. (A) The functioning of the surface-modified coating and (B) the antimicrobial activity of the coating.

1.10 The use of nanoparticles as antimicrobial materials

Recent advances in the field of nanotechnology led several groups to recognize the promise of recruiting nanomaterials to the ongoing battle against pathogenic bacteria. A large battery of newly discovered and developed nanomaterials has been accumulating during the last decade, therefore, it could be anticipated that it should only be a matter of time until such preliminary nanomedicine applications will be made available. Indeed, the increased development of bacterial resistance to traditional antibiotics has created a great need for the development of new

antimicrobial agents. Nanotherapeutics has lately evoked tremendous interest in controlling the development of oral biofilms by the use of biocidal nanoparticles (NPs). Treatment with conventional antibiotics is considered inadequate, and often leads to chronic oral infections, which compel tooth extractions or implant removal, involving costly restoration or regenerative procedures [57].

The application of nanomaterials as new antimicrobials should provide novel modes of action and/or different cellular targets compared with existing antibiotics. The field of nanomaterials science has also provided novel materials with unique properties that make them suitable for the encapsulation of active molecules that may be harnessed for antimicrobial applications [58]. Two groups of antibacterial nanomedicines have been defined: the first are compounds derived from artificial synthetic materials [58]; whereas the second comprises materials based on natural biological compounds [58].

It is important to recognize that while some metals, such as zinc, silver, and copper, exhibit antibacterial mechanisms in their bulk form, other materials, such as iron oxide, are not antibacterial in their bulk form but may exhibit antibacterial properties in nanoparticulate form [59].

The mechanism of this antibacterial activity varies from nanoparticle to nanoparticle. For all varieties of nanoparticles, the antibacterial mechanism is not fully understood. While some proposed mechanisms relate to the physical structure of the nanoparticles (ie, membrane-damaging abrasiveness of the nanoparticle), others relate to the enhanced release of antibacterial metal ions from nanoparticle surfaces [59]. The specific surface area of a dose of nanoparticles increases as the particle size decreases, allowing for greater material interaction with the surrounding environment. Comparing results across a greater number of studies allows for the identification of nanoparticle parameters which are most relevant in designing the ideal antibacterial particle (Table 1). Chemistry, particle size, particle shape, and zeta potential are among the most relevant variables affecting antibacterial activity [59].

Table 1.1 Summary of selected studies concerning the antimicrobial effects of nanoparticles. Table 1.1 adopted from [56].

Chemistry	Size (average)	Zeta potential	Organism tested	MIC	Proposed mechanism
ZnO	13 nm	N/A	<i>Staphylococcus aureus</i>	Reduced 95% at 80 µg/mL	ROS inhibition
ZnO	60 nm	N/A	<i>S. aureus</i>	Reduced 50% at 400 µg/mL	ROS inhibition
ZnO	40 nm	Positive (no value)	<i>S. aureus</i> , <i>Escherichia coli</i>	Both species reduced 99% at 400 µg/mL	Membrane disruption
ZnO	12 nm	N/A	<i>E. coli</i>	Reduced 90% at 400 µg/mL	Membrane damage due to particle abrasiveness
ZnO ions	N/A	N/A	<i>Pseudomonas aeruginosa</i> , <i>S. aureus</i> , <i>Candida albicans</i>	Reduced 100% at 1917, 9, and 39 µg/mL, respectively	ROS inhibition
Silver	21 nm	N/A	<i>E. coli</i> , <i>Vibrio cholerae</i> , <i>Salmonella typhi</i> , <i>P. aeruginosa</i>	All reduced 100% at 75 µg/mL	Membrane disruption, Ag ion interference with DNA replication
Silver	Triangles (50 nm)	Positive (no value, cationic surfactant)	<i>E. coli</i>	Reduced 99% with 0.1 µg/mL added to agar surface	Membrane disruption, Ag ion interference with DNA replication
Silver	12 nm	Negative (no value)	<i>E. coli</i>	Reduced 70% with 10 µg/mL in agar	Membrane disruption, Ag ion interference with DNA replication
Silver	13.5 nm	-0.33 mV	<i>S. aureus</i> , <i>E. coli</i>	Inhibitory concentration of 3.56 µg/L and 0.356 µg/L, respectively, added to agar surface	Membrane disruption, Ag ion interference with DNA replication
Cu	100 nm	N/A	<i>E. coli</i> , <i>Bacillus subtilis</i>	Reduced 90% at 33.40 µg/mL and 28.20 µg/mL, respectively	Protein inactivation via thiol interaction
Fe ₃ O ₄	9 nm	-19.09 mV	<i>S. aureus</i>	Increased dead cells observed at 3 mg/mL	ROS, membrane disruption
Fe ₃ O ₄	8 nm	N/A	<i>Staphylococcus epidermidis</i>	Reduced 65% at 2 mg/mL	ROS, membrane disruption
Al ₂ O ₃	11 nm	120 mV	<i>E. coli</i>	Reduced 35%, 70%, and 68% at 10, 100, and 500 µg/mL, respectively	Dose-dependent ROS, particle penetration
Al ₂ O ₃	60 nm	30 mV	<i>E. coli</i> , <i>B. subtilis</i> , <i>Pseudomonas fluorescens</i>	Reduced bacteria species by 36%, 57%, and 70% at 20 µg/mL	Flocculation
TiO ₂	17 nm	12 mV	<i>E. coli</i>	Reduced 0%, 35%, and 80% with 10, 100, and 500 µg/mL, respectively	Membrane disruption
SiO ₂	20 nm	35 mV	<i>E. coli</i> , <i>B. subtilis</i> , <i>P. fluorescens</i>	Reduced bacteria species 58%, 40%, and 70% at 20 µg/mL	Flocculation, membrane disruption
Chitosan	40 nm	51 mV	<i>E. coli</i> , <i>S. aureus</i>	Reduced bacteria species 100% at 4 µg/mL and 8 µg/mL, respectively	Flocculation, membrane disruption

1.10.1 The Use of Nanoparticles to Control Oral Biofilm Formation

Issues surrounding the uptake and penetration of antimicrobial agents into biofilms are key considerations in the administration of therapeutics [60,61]. This is of particular importance within the oral cavity when these agents have to reach less accessible stagnation sites or through plaque to the enamel. Thus, there remains an

interest in the development of plaque control measures that require a minimum of public compliance and professional healthcare intervention [62]. Antimicrobial nanoparticles may be of particular value if retained at approximal tooth surfaces and below the gum margin. The anti-caries potential of fluoride and other more conventional antimicrobial/antiplaque agents, which are mostly deployed in mouthwashes and toothpastes, have received the greatest attention to date [63]. However, the potential of nanoparticles as constituents of topical agents to control oral biofilms through either their biocidal or anti-adhesive capabilities is now emerging as an area worthy of serious consideration. The studies by Robinson and co-workers using the 'Leeds in situ model', a device to generate dental plaque in situ on a removable human enamel surface, have helped in the assessment of novel antimicrobial agents and take into account the very complex microbial composition and architecture of plaque biofilms [64]. The use of such intact biofilms on natural tooth surfaces would be of particular value for study of the penetration of nanoparticles and released ions in situ. The use of this model has demonstrated that plaque contains voids and channels, sometimes extending completely through the biomass to the underlying enamel [65]. Such channels may have considerable influence on the transfer of nanoparticles through biofilms. Thus, the main considerations are the physico-chemical characteristics of the particular nanoparticles used, including the surface charge and degree of hydrophobicity, the surface-area-to-mass ratio of the plaque biofilm, and the ability of the particles to adsorb to/be taken up at the biofilm surface. Within this context, nanoparticles are potentially useful because it is possible to alter their surface charge, hydrophobicity, and other physical and chemical characteristics [66].

1.10.1.1 Metal oxide

Research in the area of nanometer-scaled metal oxides has shown encouraging discoveries that have demonstrated a clear size dependence of their electromagnetic, optical, and catalytic properties [67,68]. One striking characteristic of nanometer-scaled metal oxides is their broad range of probable reactions with the biological cells in general and with bacterial cells in particular [69,70]. Metal oxide nanoparticles (NPs), as antimicrobial agents, can fulfill the need of a new class of biocidal formulations. Moreover, metal oxide NPs have the key advantage that they are

inorganic materials and, therefore, hold the ability to withstand adverse processing conditions [71]. They can be prepared with extremely high surface areas and unusual crystal morphologies that have a high number of edges and corners, and other potentially reactive sites [72].

1.10.1.1.1 Zinc oxide NPs

Zinc oxide (ZnO) has been the topic of high-standard contemporary research because of its wide band gap (3.37 eV) and large exciton-binding energy (60 meV) that cause interesting luminescent, piezoelectric, and photoconducting properties. These properties make this material suitable for many industrial applications in fields such as high frequency surface devices, optical devices, such as UV detector, LDs, and LEDs, and which increasingly attracting more research groups [73-76]. ZnO is an environmentally friendly material and has little toxicity, which is why it is widely used as an active ingredient for dermatological applications in creams, lotions and for personal care products [77,78]. ZnO NPs showed excellent antimicrobial properties and, unlike silver, exhibit no toxicity to human cells [79,80]. Nanoparticles of ZnO are currently being investigated as antibacterial agents in microscale and nanoscale formulations for both Gram-negative (e.g. *E. coli*) and Gram-positive (e.g. *S. aureus*) microorganisms [81]. ZnO has been shown to naturally reduce the activity of a wide range of (mostly Gram-positive) bacteria strains without the use of antibiotics [82]. ZnO and several other oxide powders have been specifically shown to kill several oral microbes known to contribute to caries [83]. Smaller particles of ZnO nanoparticles (NPs) have been found to be more effective than larger particles against both gram negative and gram positive bacteria [84,85]. The mechanism of the antibacterial activity of ZnO is interpreted by reactive-oxygen-species (ROS) production and oxidative injury inside bacterial cells has become an established paradigm underlying the ZnO antibacterial mechanism [86].

1.10.1.1.2 Copper oxide NPs

Among the large family of metal oxides, cupric oxide (CuO) is an interesting multifunctional material due to its promising applications in magnetic storage media, solar energy transformation, electronics, sensors, batteries and catalysis. Cupric oxide

is cheaper than silver, easily mixed with polymers and relatively stable in terms of both chemical and physical properties [87].

CuO has proven efficacy toward various microorganisms including yeast [88], bacteria [89] and even viruses [90], the exploitation of copper oxide ranges widely from wood preservation [91], antifouling paints, to antibacterial textiles [92]. In its nano form (<100 nm), copper oxide displays enhanced antimicrobial activity toward a broad spectrum of microorganisms, including pathogens such as *Escherichia coli* and *Staphylococcus aureus* [93]. Recent studies have identified the leaching characteristics of nanoparticles as one of the key properties leading to their antimicrobial efficacy (or a wider context of nanotoxicity) [94,95]. Leached nanoparticles in the form of soluble ions interact directly with the cellular membrane or are taken up intracellularly, thereby causing cytotoxicity. Alternatively, the Trojan horse effect, whereby nanoparticles are internalized and dissolved intracellularly, has been suggested [94,96]. Or the intracellular generation of reactive oxygen species (ROS), a general oxidative stress.

1.11 Biochemical actions of fluoride on oral biofilm

Dental caries is essentially a disease of demineralization. Considerable data support fluoride uptake as a remedy to demineralization by acting as an active agent in remineralization [97]. The electrostatic interaction between Ca^{+2} and the F^- is greater than that between Ca^{+2} and OH^- ions, making the fluoridated apatite lattice more crystalline and more stable [98]. As a consequence, it becomes less soluble in acid [99]. The direct topical administration of fluoride on the tooth after its eruption appears more effective than its intake in the diet [100]. It is therefore the most important component in toothpastes and mouthwashes. Fluorides may also inhibit bacterial metabolism. Fluorine in the ionic form (F^-) cannot cross the cell wall and membrane of bacteria, but can be taken up readily as HF [101]. When the pH in the plaque falls, a portion of the F^- ions combines with hydrogen ions to form HF and diffuses into the cell. After entry into the cell, HF acidifies the cell and dissociates, thereby releasing F^- ions. F^- ions are toxic to cells as they interfere with the enzyme machinery of the cell [97,101].

1.11.1 Biochemical actions of fluoride on microorganisms

(i) Actions dependent on direct binding of F⁻/HF. The most direct mode of action for fluoride involves binding of F⁻ or HF to specific sites of enzymes or other proteins, for example the heme components of a variety of enzymes. In many instances, F⁻ binds to sites that would normally bind OH⁻ and subsequently a proton, in a way very similar to the binding of F⁻ to apatites in teeth with resultant formation of fluoroapatites instead of the normal hydroxylapatites[102].

Fluoride inhibition of enzymes and regulatory proteins may be important physiologically for intact organisms. For example, enolase inhibition is considered to be important in fluoride inhibition of glycolysis by intact cells, and this inhibition can occur at low fluoride concentrations down to the micromolar level in acidified environments[103]. In addition, fluoride inhibition of catalase has been shown to be important in compromising the capacities of intact bacteria of mixed communities in acid environments to cope with oxidative damage from hydrogen peroxide [104]. It is important to emphasize that fluoride binding is enhanced by acidification.

(ii) Metal complexes and effects on phosphoryl transfer. The importance of metal-fluoride complexes, especially AlF₄⁻ or BeF₃⁻ • H₂O, as modulators of enzymes activities and metabolic regulation was initially reported by Sternweis and Gilman[105]. Studies showed that beryllium could be as effective as aluminum in serving as a partner for fluoride and that the effectiveness of the complexes could be related to their acting as mimics for phosphate. The complexes have been extensively studied in terms of their abilities to affect phosphatase enzymes, such as F-ATPases[106]. Furthermore, metal-fluoride complexes involved in inhibition of acetate kinase (MgADP-aluminium-fluoride-acetate complex)[107], sensor kinases such as RecA (ADP-AlF₄ complex)[108] and CheY (BeF₃⁻ complex)[109] proteins, regulatory proteins such as NtrC (ADP•BeF_x complex)[110], and nitrogenase (MgADP)[111] were also reported.

(iii) Action as transmembrane proton carrier. Fluoride in the form of HF acts to convey protons across the membranes of living bacteria and to diminish ΔpH across the cell membrane. The transport of protons into cells in acidified environments acts against the functioning of the F-ATPase to move protons out of the cytoplasm [112].

1.12 Sonochemical synthesis

1.12.1 Introduction

Sonochemistry [113] is the research area in which molecules undergo a chemical reaction due to the application of powerful ultrasound radiation (20 kHz–10 MHz). The physical phenomenon responsible for the sonochemical process is acoustic cavitation.

The main event in sonochemistry is the creation, growth, and collapse of a bubble that is formed in the liquid. The stage leading to the growth of the bubble occurs through the diffusion of solute vapor into the volume of the bubble. The last stage is the collapse of the bubble, which occurs when the bubble size reaches its maximum value. During the collapse very high temperatures (5000–25,000 K) [114] are obtained and causing the breaking of chemical bonds. Since this collapse occurs in less than a nanosecond [115], very high cooling rates, in excess of 10¹¹ K/s, are also obtained. This high cooling rate hinders the organization and crystallization of the products. For this reason, in all cases dealing with volatile precursors where gas phase reactions are predominant, amorphous nanoparticles are obtained. The explanations for the formation of nanostructures are that the fast kinetics does not permit the growth of the nuclei, and in each collapsing bubble a few nucleation centers are formed whose growth is limited by the short collapse. If, on the other hand, the precursor is a non-volatile compound, the reaction occurs in a 200 nm ring surrounding the collapsing bubble [116]. The temperature in this ring is in the region as 1900°C [117], which it is lower than inside the collapsing bubble, but higher than the temperature of the bulk. In almost all the sonochemical reactions leading to inorganic products, nanomaterials were obtained. They varied in size, shape, structure, and in their solid phase (amorphous or crystalline), but they were always of nanometer size.

TiO₂ has been synthesized by the hydrolysis of titanium tetra-isopropoxide while sonicating the mixture of tetra-isopropoxide (TTIP) in the presence of de-ionized water, ethanol, and acetic acid [118]. Fe₂O₃ was synthesized [119] using Fe(CO)₅ in decalin and was irradiated with a high intensity ultrasonic horn under 1.5 atm of air at 0 °C for 3 h, then the sample was heated to 130 °C under vacuum or under argon for 3 h. Moreover, ZnO was synthesized [120] by the following procedure: an aqueous ZnCl₂ solution was added to an aqueous KOH solution within about 30 min and

sonicated for 2 h. Metal Oxides are also synthesized from Metal Acetates [121], zinc(II) acetate dihydrate and copper(II) acetate monohydrate are added to doubly distilled deoxygenated water or 10% water-DMF is irradiated with a high-intensity ultrasonic horn under 1.5 atm of argon at room temperature for 3 h.

1.12.2. Sound, Ultrasound, and Cavitation

Sound is nothing more than waves of compression and expansion passing through gases, liquids or solids. We can sense these waves directly through our ears if they have frequencies from about Hertz to 16 kHz. These frequencies are similar to low frequency radio waves, but sound is intrinsically different from radio or other electromagnetic radiation. For example, electromagnetic radiation (radio waves, infrared, visible light, ultraviolet, x-rays, gamma rays) can pass through a vacuum without difficulty; on the other hand, sound cannot because the compression and expansion waves of sound must be contained in some form of matter. High intensity sound and ultrasound are generally produced in a similar fashion: electric energy is used to cause the motion of a solid surface, such as a speaker coil or a piezoelectric ceramic. Piezoelectric materials expand and contract when an electric field is applied.

For ultrasound, a high frequency alternating electric current is applied to a piezoelectric attached to the wall of a metal container. Ultrasound can easily be introduced into a chemical reaction in which there is good control of temperature and ambient atmosphere. The titanium rod shown immersed in the reaction liquid is driven into vibration by a piezoelectric, which vibrates when subjected to an alternating current electric field. The usual piezoelectric ceramic is PZT, a lead zirconate titanate material. Ultrasound has frequencies pitched above human hearing (above roughly 16 kHz). Scientists can make narrow beams of "silent" ultrasound far more intense than the roar of a jet engine, but completely unheard by our ears. Ultrasound has wavelengths between succession compression waves measuring roughly 10 cm to 10^{-3} centimeters. These are not comparable to molecular dimensions. Because of this mismatch, the chemical effects of ultrasound cannot result from a direct interaction of sound with molecular species. Nonetheless, the ultrasonic irradiation of liquids does produce a plethora of high energy chemical reactions. This occurs because ultrasound causes other physical phenomena in liquids that create the conditions necessary to drive chemical reactions. The most important

of these is cavitation: the formation, growth, and implosive collapse of bubbles in a liquid. The dynamics of cavity growth and collapse are strikingly dependent on the local environment. Cavity collapse in a homogeneous liquid is very different from cavitation near a liquid-solid interface, which will be considered later. As ultrasound passes through a liquid, the expansion cycles exert a negative pressure on the liquid, pulling the molecules away from one another. If the ultrasound is sufficiently intense, the expansion cycle can create cavities in the liquid. This will occur when the negative pressure exceeds the local tensile strength of the liquid, which varies according to the type and purity of liquid. Normally, cavitation is a nucleated process; that is, it occurs at pre-existing weak points in the liquid, such as gas-filled crevices in suspended particulate matter or transient microbubbles from prior cavitation events. Most liquids are sufficiently contaminated by small particles that cavitation can be readily initiated at moderate negative pressures. Once formed, small gas bubbles irradiated with ultrasound will absorb energy from the sound waves and grow. Cavity growth depends on the intensity of the sound. At high intensities, a small cavity may grow rapidly through inertial effects. If cavity expansion is sufficiently rapid during the expansion half of a single cycle, it will not have time to recompress during the compression half of the acoustic cycle. At lower acoustic intensities cavity growth can also occur by a slower process called rectified diffusion (Figure 1.9). Under these conditions, a cavity will oscillate in size over many expansion and compression cycles. During such oscillations the amount of gas or vapor that diffuses in or out of the cavity depends on the surface area, which is slightly larger during expansion than during compression. Cavity growth during each expansion is, therefore, slightly larger than shrinkage during the compression. Thus, over many acoustic cycles, the cavity will grow. The growing cavity can eventually reach a critical size where it can efficiently absorb energy from the ultrasonic irradiation. Called the resonant size, this critical size depends on the liquid and the frequency of sound; at 20 kHz, for example, it is roughly 170 micrometers. At this point, the cavity can grow rapidly during a single cycle of sound. Once the cavity has overgrown, either at high or low sonic intensities, it can no longer absorb energy as efficiently. Without the energy input the cavity can no longer sustain itself. The surrounding liquid rushes in, and the cavity implodes. It is the implosion of the cavity that creates an unusual environment for chemical reactions.

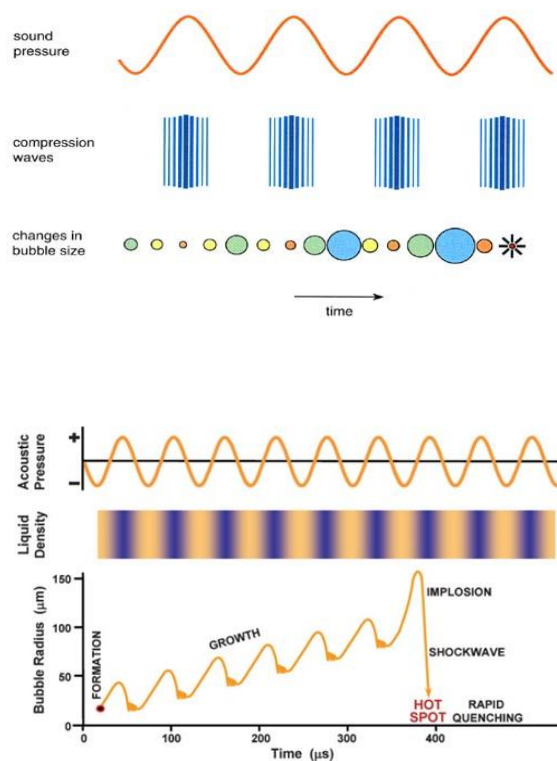


Figure 1.11. Bubble growth and implosion. Bubble growth and implosion in a liquid irradiated with ultrasound is the physical phenomenon responsible for most sonochemistry. Intense ultrasound waves generate large alternating stresses within a liquid by creating regions of positive pressure (blue color) and negative pressure (orange color). A cavity can form and grow during the episodes of negative pressure. When the cavity attains a critical size, the cavity implodes, generating intense heat and tremendous pressure.

1.12.3 The Sonochemical Hot-Spot

Compression of a gas generates heat. On a macroscopic scale, one can feel this when pumping a bicycle tire; the mechanical energy of pumping is converted into heat as the tire is pressurized. The compression of cavities when they implode in irradiated liquids is so rapid that little heat can escape from the cavity during collapse. The surrounding liquid, however, is still cold and will quickly quench the heated cavity. Thus, one generates a short-lived, localized hot spot in an otherwise cold liquid. Such a hot spot is the source of homogeneous sonochemistry; it has a temperature of roughly 5000° C (9,000° F), a pressure of about 1000 atmospheres, a lifetime considerably less than a microsecond, and heating and cooling rates above

10 billion °C per second. For a rough comparison, these are, respectively, the temperature of the surface of the sun, the pressure at the bottom of the ocean, the lifetime of a lightning strike, and a million times faster cooling than a red hot iron rod plunged into water! Thus, cavitation serves as a means of concentrating the diffuse energy of sound into a chemically useful form. Alternative mechanisms involving electrical microdischarge have been proposed (most recently by M.A. Margulis of the Russian Institute for Organic Synthesis) [122], but they do not appear fully consistent with observed data. Determination of the temperatures reached in a cavitating bubble has remained a difficult experimental problem. The transient nature of the cavitation event precludes direct measurement of the conditions generated during bubble collapse. Chemical reactions themselves, however, can be used to probe reaction conditions. The effective temperature of a system can be determined with the use of competing unimolecular reactions whose rate dependencies on temperature have already been measured. This technique of "comparative-rate chemical thermometry" was used by K.S. Suslick, D.A. Hammerton and R.E. Cline, Jr., at the University of Illinois to determine the effective temperature reached during cavity collapse [123]. For a series of organometallic reactions, the relative sonochemical rates were measured. In combination with the known temperature behavior of these reactions, the conditions present during cavity collapse could then be determined. The effective temperature of these hot spots was 5,200 K. Of course, the comparative rate data represent only a composite temperature: during the collapse, the temperature has a highly dynamic profile, as well as a spatial gradient in the surrounding liquid. When a liquid is subjected to ultrasound, not only does chemistry occur, but light is also produced. Such "sonoluminescence" provides an alternate measure of the temperature of the high-energy species produced during cavitation. High-resolution sonoluminescence spectra were recently reported and analyzed by E.B. Flint and Suslick [124]. From a comparison of synthetic to observed spectra, the effective cavitation temperature of the emitting species is 5,100 K. The agreement between this spectroscopic determination of the cavitation temperature and that made by comparative rate thermometry of sonochemical reactions is surprisingly close.

1.12.4 Sonochemistry in nanomaterial synthesis

Sonochemistry is the research area in which molecules undergo chemical reaction due to the application of powerful ultrasound radiation (20 KHz - 10 MHz)

[125,126]. The physical phenomenon responsible for the sonochemical process is acoustic cavitation. A number of theories have been developed in order to explain how 20 kHz sonic radiation can break chemical bonds. They all agree that the main event in sonochemistry is the creation, growth, and collapse of a bubble that is formed in the liquid [126].

The first question is how such a bubble can be formed, considering the fact that the forces required to separate water molecules to a distance of two van-der Waals radii, would require a power of 10^5 W/cm [125,126]. On the other hand, it is well known that in a sonication bath, with a power of 0.3 W/cm, water is already converted into hydrogen peroxide [125,126]. Different explanations have been offered; they are all based on the existence of unseen particles, or gas bubbles, that decrease the intermolecular forces, enabling the creation of the bubble [125,126]. The experimental evidence for the importance of unseen particles in sonochemistry is that when the solution undergoes ultra filtration, before the application of the ultrasonic power, there is no chemical reaction and chemical bonds are not ruptured [126].

The second stage is the growth of the bubble, which occurs through the diffusion of solute vapor into the volume of the bubble. The third stage is the collapse of the bubble, which occurs when the bubble size reaches its maximum value [125,126].

One of the theories that explain why, upon the collapse of a bubble, chemical bonds are broken is the "hot spot mechanism". The theory claims that very high temperatures (5,000-25,000 K) are obtained upon the collapse of the bubble [125,126]. Since this collapse occurs in less than a nanosecond, very high cooling rates, in excess of 10^{11} K/S, are obtained. This high cooling rate hinders the organization and crystallization of the products [126]. For this reason, in all cases dealing with volatile precursors, where gas phase reactions are predominant, amorphous NPs are obtained. While the explanation for the creation of amorphous products is well understood, the reason for the nanostructured products is not clear [126]. One explanation is that the fast kinetics does not permit the growth of the nuclei. If, on the other hand, the precursor is a non-volatile compound, the reaction occurs in a 200 nm ring surrounding the collapsing bubble [126,127]. In this case, the sonochemical reaction occurs in the liquid phase [126,127]. The products are sometimes nanoamorphous particles, and in other cases, nanocrystalline [126,127].

This depends on the temperature in the ring region where the reaction takes place. The temperature in this ring is lower than inside the collapsing bubble, but higher than the temperature of the bulk. Suslick has estimated the temperature in the ring region as 1900 °C [125]. In short, in almost all the sonochemical reactions leading to inorganic products, nanomaterials were obtained. They varied in size, shape, structure, and in their solid phase (amorphous or crystalline), but they were always of nanometer size [126].

One important parameter in the sonication process is the temperature. The equation (1) of an adiabatic implosion is

$$(1) T_{\max} = T_0 \{ P_{\text{ex}} (\gamma - 1) / P_{\text{bub}} \}$$

where T_{\max} is the temperature reached after the collapse of the bubble, T_0 is the temperature of the sonication bath, $\gamma = C_p/C_v$, P_{ex} is the external pressure equal to the sum of the hydrostatic and acoustic pressure, and P_{bub} is the pressure of the gas inside the cavity, at the radius at which it collapses. The choice of a nonvolatile solvent (such as decalin, hexadecane, isodurene, etc.) guarantees that only the vapors of the solute can be found inside the cavitating bubble. Thus, P_{bub} is practically the vapor pressure of the solute, and since it is found in the denominator, lower P_{bub} results in higher temperatures and faster reaction rates. The conclusion is that the temperature affects the sonochemical reaction rate in two ways. On the one hand, lower temperatures cause a higher viscosity [126], which makes the formation of the bubble more difficult, and, on the other hand, the dominant effect is that at lower temperatures, higher rates will be achieved in sonochemical processes [126]. This is why the sonic reaction involving volatile precursors is run at lower temperatures. Apparent negative activation energies were measured for sonochemical reactions [126].

2. Research Objectives

2.1 Research importance

The use of antibiotic treatments became ineffective due to the development of strains of bacteria with resistance to many types of antibiotics. Moreover, the inherent resistance of biofilms to killing and their pervasive involvement in implant-related infections has prompted the search for surfaces/coatings that inhibit bacterial colonization. One approach comes from recent progresses in nanotechnology, which offers an opportunity for the discovery of compounds with antimicrobial activity as well as the use of "nano-functionalization" surface techniques. Therefore, this study developed a novel approach which combines nanotechnology with antibacterial/antibiofilm applications. The motivation is to develop effective methods for preparing nanoparticles and their stable coatings on surfaces, as well as to understand the mechanisms of these antibacterial/antibiofilm nanoparticles.

The present study examined the capability of ZnO, CuO, Zn-CuO and MgF₂ NPs which were prepared by sonochemical-assisted processes to inhibit *Streptococcus mutans* (which has a well-known role in the development of dental caries) biofilm formation on teeth model. Our results in this research suggest a promising strategy for antibiofilm activity that can be further developed to improve oral health.

2.2 Research goals

2.2.1 Major goals

Synthesis and coating of metal oxide and metal fluoride nanoparticles on tooth surfaces by using the sonochemistry method, and understanding their antibacterial/antibiofilm activities against *S. mutans* bacteria.

2.2.2 Minor goals

1. Synthesis of nanomaterials with intrinsic antibacterial properties such as (ZnO, CuO, Zn-CuO and MgF₂) by ultrasound irradiation. These nanomaterials were characterized using standard methodology.
2. These as-prepared NPs were tested for their antimicrobial properties toward *Streptococcus mutans*, well known oral bacteria.

3. Optimization of the coating process parameters for all the different nano particles (selection of the reaction time, temperature, concentration for reactants, reaction atmosphere *etc.*) in order to obtain a uniform and stable coating over the entire tooth surface. The tooth surface was characterized by different techniques such as, HR-SEM, FIB and RBS.
4. Understanding the antibacterial and antibiofilm activities of all different nano particles against *S. mutans* bacteria.
5. Examination of the leaching of nanoparticles and/or ions from NPs and from coated teeth in various environments.

2.3 Novelty of the Research

The novelty of my research encompasses the synthesis, characterization and properties of various nanomaterials such as MgF_2 , metal oxides (ZnO, CuO, and Zn-CuO) and their deposition on teeth by using sonochemistry. The original concept of applying sonochemistry to the coating of teeth is developed and reported in the current thesis. To the best of our knowledge, this work is the first to present the use of ultrasound irradiation for the synthesis and deposition of nanoparticles on teeth. In the literature there are few reports dealing with ZnO and CuO NPs for preventing *S. mutans* biofilm. In any case, none of them report on coating teeth via the sonication route.

Moreover, we have shown that CuO NPs did not reveal antibacterial activity against *S. mutans* bacteria. In our comparison study between CuO and Zn-CuO NPs, surprisingly, the Zn-doped CuO composite NPs (Zn-CuO) were found to have some antibacterial activity against *S. mutans* bacteria which finally lead to enhancement in its antibiofilm activity as well. To the best of our knowledge, the antibacterial and antibiofilm activities of Zn-doped CuO against *S. mutans* has not yet been reported. In fact, there are almost no studies regarding the antibacterial and antibiofilm activities of doped or mixed metal oxides.

In addition, in the case of MgF_2 , fluoride ions (unlike metal oxides) are commonly used in oral healthcare and thus can provide a much more attractive approach to coat the surfaces of teeth and utilized as an antibiofilm agent. We have not shown so far the ability of MgF_2 to block biofilm formation of oral pathogens and

as far as we know, there are no publications dealing with nanoparticles of MgF_2 for avoiding oral biofilm.

3- Experimental System

The research includes synthesis and deposition method of different nanoparticles on teeth surface:

1. ZnO NPs

2. CuO NPs
3. $\text{Cu}_{0.88}\text{Zn}_{0.12}\text{O}$, (noted Zn-CuO)- Zn-doped CuO composite
4. MgF_2 NPs

This section summarizes the optimal experimental conditions for coating teeth with nanoparticles in a one-step reaction using the sonochemistry method.

3.1 Teeth used in this research

The artificial acryl teeth (Figure 3.1) were obtained from the School of Dental Medicine at the Tel Aviv University.



Figure 3.1. Artificial acryl teeth.

3.2 Synthesis of NP coated teeth

NP coatings were obtained by placing an artificial acryl tooth directly into the sonochemical reaction medium. The tooth was held by a wire in order to keep it at a constant distance of 2 cm from the sonicator's tip during the entire reaction process (Figure 3.2).

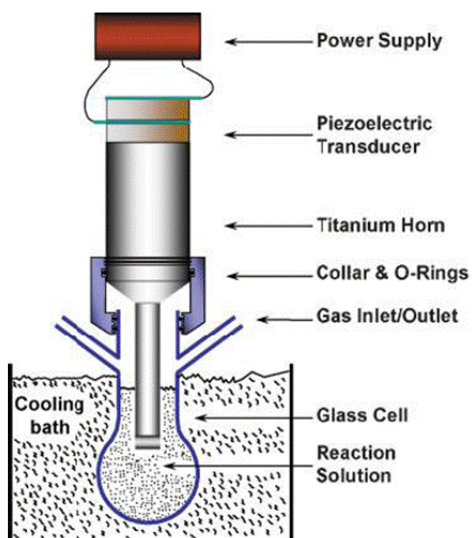


Figure 3.2. Experimental setup for sonochemical reaction.

3.2.1 ZnO and CuO NPs synthesis and coating procedure

0.02 g of zinc acetate, $[\text{Zn}(\text{O}_2\text{CCH}_3)_2 \cdot 2\text{H}_2\text{O}]$ or copper acetate $[\text{Cu}_2(\text{OAc})_4 \cdot \text{H}_2\text{O}]$ (purchased from Aldrich and used without further purification) were dissolved in 10 mL of double-distilled water (ddH₂O). To this solution ethanol was added for a final volume of 100 mL with an ethanol/water ratio of 10:1. In order to achieve a basic pH, $\text{NH}_3 \cdot \text{H}_2\text{O}$ were added until the pH value of the solution was ~8. The reaction mixture was irradiated for 30 min with a high-intensity ultrasonic horn (Ti horn, 20 kHz, 750 W at 60% efficiency). The sonication vessel was placed in a cooling bath, maintaining a constant temperature of 30 °C during the reaction. The obtained solution was centrifuged and the resulting precipitating products were washed twice with ddH₂O and then with ethanol, then the obtained NPs were dried under a vacuum.

NP coatings were obtained by placing an artificial acryl tooth (teeth were obtained from the School of Dental Medicine at the Tel Aviv University) directly into the sonochemical reaction medium according to the methodology described above. The tooth was held by a wire in order to keep it at a constant distance of 2 cm from the sonicator's tip during the entire reaction process.

3.2.2 Zn-CuO NPs synthesis and coating procedure

To obtain the, $\text{Cu}_{0.88}\text{Zn}_{0.12}\text{O}$, Zn-CuO NPs, The molar ratio of reagents zinc and copper acetates in the aqueous solution was Cu:Zn 3:1. Copper acetate monohydrate was dissolved in 10 ml of double distilled water by stirring, after which, zinc acetate dihydrate was added. The concentrations of Cu^{+2} and Zn^{+2} were 0.0075M and 0.0025M, respectively. To this solution ethanol was added to a final volume of 100 mL. After 5 min of sonication, 0.8 ml of an aqueous solution of ammonium hydroxide (28%-30%) was injected into the reaction cell to adjust the pH to ~8. The working solution was chilled in a water bath, keeping the temperature at 30°C. The

sonochemical deposition process continued for 30 min with a high-intensity ultrasonic horn (Ti horn, 20 kHz, 750 W at 60% efficiency). The identification of the product as $\text{Cu}_{0.88}\text{Zn}_{0.12}\text{O}$ is found elsewhere [128].

The obtained solution was centrifuged and the resulting precipitating products were washed twice with ddH_2O and then with ethanol, after which the obtained NPs were dried under vacuum.

NP coatings were obtained by placing an artificial acryl tooth (teeth were obtained from the School of Dental Medicine at the Tel Aviv University) directly into the sonochemical reaction medium according to the methodology described above. The tooth was held by a wire in order to keep it at a constant distance of 2 cm from the sonicator's tip during the entire reaction process.

3.2.3 MgF_2 synthesis and coating procedure

Magnesium (II) acetate tetrahydrate ($[\text{Mg}(\text{Ac})_2 \cdot \text{H}_2\text{O}]_4$), Aldrich, Rehovot, Israel, 99% purity) and concentrated hydrofluoric acid (HF, 32% weight aqueous solution, ACS grade, BioLab, Jerusalem, Israel) were dissolved in double-distilled water ddH_2O , (100 mL) at a 1:2 equivalent ratio for Mg:F. The reaction mixture was irradiated for 60 min with a high-intensity ultrasonic horn (Ti horn, 20 kHz, 750 W at 60% efficiency). NP coatings were obtained by placing an artificial acryl tooth (teeth were obtained from the School of Dental Medicine at the Tel Aviv University) directly into the sonochemical reaction medium according to the methodology described above. The tooth was held by a wire in order to keep it at a constant distance of 2 cm from the sonicator's tip during the entire reaction process.

3.3 Characterization methods

3.3.1 Transmission Electron Microscopy (TEM)

Transmission electron microscopy (TEM) is an imaging technique in which a beam of electrons is focused onto a specimen causing an enlarged image of the sample to appear on a fluorescent screen or on a photographic film, or to be detected by a CCD camera. The first practical transmission electron microscope was built by Albert Prebus and James Hillier at the University of Toronto in 1938 using concepts developed earlier by Max Knoll and Ernst Ruska. TEM works like a slide projector. Instead of a light bulb, an electron source is used. This is either a glowing tungsten tip, a heated LaB_6 single-crystal, or a field emitter. The ejected electrons are

accelerated to approximately $2/3$ of the velocity of light, fast enough to cross samples which are less than 300 nm thick, (approximately 100 atomic layers). The image of the sample is projected using magnetic lenses onto the screen of the detector. According to the quantum theory, the high velocity and the mass of electrons yield a wave of very small wavelengths and make it possible to achieve interferences at an atomic resolution. X-ray detectors and energy filters provide element-specific signals. Chemical microanalysis on a scale of less than 1 nm has been demonstrated with sensitivity less than 10 atoms. The electrons can be focused onto the sample providing a resolution far better than what is possible with light microscopes.

3.3.2 Scanning Electron Microscopy (SEM)

SEM is designed for direct studies of solid surfaces and their imaging at high resolution. By scanning with an electron beam that is generated and focused by the operation of a microscope, an image of the probed surface is obtained using the appropriate detecting by flour scinting screen, diodes arrays etc. SEM allows a greater depth of focus than the optical microscope. For this reason, SEM can produce an image that is a good representation of the three-dimensional structure of a surface. In a typical SEM instrument, electrons are emitted from a LaB_6 cathode and are accelerated towards the anode. Alternatively, electrons can be emitted via field emission (FE). The electron beam, which typically has an energy ranging from several hundred of eV to 50 keV, is focused by one or two condenser lenses into a beam with a fine focal spot, of a 1 - 5 nm size. The beam is collimated by electromagnetic condenser lenses, focused by an objective lens, and scanned across the surface of the sample by electromagnetic deflection coils. As the primary electrons strike the surface, they are inelastically scattered by the atoms of the sample. In the primary imaging method, the secondary electrons that are released by the sample, are detected by a scintillation material that produces photons. The photons are then detected and amplified by a photomultiplier tube. By correlating the sample scan position with the resulting signal, an image can be formed that is strictly similar to what would be seen through an optical microscope. The illuminated and shadowed areas in image of the surface under the beam produce a quite natural looking surface topography. Scanning electron microscope resolutions are usually limited to around 25 Å.

3.3.3 Elemental Analysis

Two methods were employed for elemental analysis. The first is based on the combustion of the sample and the determination of the quantities of light elements like C, O, and N (this is a very sensitive method). The other method is Energy Dispersive X-ray Spectroscopy (EDS) that is based on measuring the energy and intensity distribution of X-ray signals generated by a focused electron beam. An especially important feature of this method is the possibility to measure element concentrations from the surface and from the bulk of the sample by changing the energy of the electron beam. EDS is suitable for heavier elements analysis, but it has very poor sensitivity for light elements like carbon. In 1913, H.G.J. Mosley showed the relationship between the atomic number (Z) and the reciprocal of the wavelength ($1/\lambda$) for each spectral series of emission lines for each element. This relationship is expressed as:

$c/\lambda = a(Z - \sigma)^2$ where "a" is a proportionality constant and " σ " is a constant dependent on a periodic series.

3.3.4 Inductively coupled plasma (ICP)

ICP is an analytical atomic spectrometer. It can identify most of the elements (except of H, N, O, C, F) and quantify their concentration in ppm units (mg/liter). The analysis is performed in aqueous homogeneous media.

3.3.5 Rutherford Backscattering Spectrometry (RBS)

RBS is one of the standard ion beam analysis techniques to determine fully quantitative depth profiles of the elemental composition of a sample surface. It relies on the fact that the energy of a backscattered light particle is a function of the mass of the sample atom. Depth information is gained via the energy loss of the ions on their way through the material. In standard RBS 2 MeV He ions are used as projectiles and backscattered particles are detected with a silicon detector. All elements from Be to U can be detected. Detection limits depend on the sample composition and are orders of magnitude better for heavy elements than for light elements such as oxygen.

3.3.6 Electron spin resonance spectroscopy (ESR)

Electron spin resonance (ESR) or electron paramagnetic resonance is a branch of absorption spectroscopy in which radiation of microwave frequency induces transitions between magnetic energy levels of electrons with unpaired spins.⁶⁷

Magnetic energy splitting is created by a static magnetic field. Unpaired electrons, relatively unusual in occurrence, are present in odd molecules, free radicals, triplet electronic states, and transition metal and rare earth ions. There is much interest in the unpaired electrons of free radicals. These electrons are generally left after hemolytic fission of a covalent bond, which is often produced by ultraviolet or gamma irradiation of the sample.

3.3.7 Confocal Microscopy

Confocal microscopy is an optical imaging technique used to increase optical resolution and contrast of a micrograph by using point illumination and a spatial pinhole to eliminate out-of-focus light in specimens that are thicker than the focal plane. It enables the reconstruction of three-dimensional structures from the obtained images. This technique has gained popularity in the scientific and industrial communities and typical applications are in life sciences, semiconductor inspection and materials science. Confocal microscopy offers several advantages over conventional optical microscopy, including controllable depth of field, the elimination of image degrading out-of-focus information, and the ability to collect serial optical sections from thick specimens.

3.3.8 Atomic Force Microscope (AFM)

The Atomic Force Microscope was developed to overcome a basic drawback with STM - that it can only image conducting or semiconducting surfaces. The AFM, however, has the advantage of imaging almost any type of surface, including polymers, ceramics, composites, glass, and biological samples. Today, most AFMs use a laser beam deflection system, introduced by Meyer and Amer, where a laser is reflected from the back of the reflective AFM lever and onto a position-sensitive detector. AFM tips and cantilevers are microfabricated from Si or Si₃N₄. Typical tip radius is from a few to 10s of nm. To acquire the image resolution, AFMs can generally measure the vertical and lateral deflections of the cantilever by using the optical lever. The optical lever operates by reflecting a laser beam off the cantilever. The reflected laser beam strikes a position-sensitive photo-detector consisting of four-segment photo-detector. The differences between the segments of photo-detector of signals indicate the position of the laser spot on the detector and thus the angular deflections of the cantilever.

3.3.9 Zeta potential

Zeta potential is a physical property which is exhibited by any particle in suspension. Most particles dispersed in an aqueous system will acquire a surface charge, principally either by ionization of surface groups, or adsorption of charged species. These surface charges modify the distribution of the surrounding ions, resulting in a layer around the particle that is different to the bulk solution. If the particle moves, under Brownian motion for example, this layer moves as part of the particle. The zeta potential is the potential at the point in this layer where it moves past the bulk solution. This is usually called the slipping plane. The charge at this plane will be very sensitive to the concentration and type of ions in solution. Zeta potential is measured by applying an electric field across the dispersion. Particles within the dispersion with a zeta potential will migrate toward the electrode of opposite charge with a velocity proportional to the magnitude of the zeta potential.

3.3. 10 Focused Ion Beam (FIB)

The Focused Ion Beam (FIB) tool can cut away (mill) material from a defined area with dimensions typically in square microns or deposit material onto it. Milling is achieved by accelerating concentrated gallium ions to a specific site, which etches off any exposed material, leaving a very clean hole or surface. By introducing gases or an organic gas compound, the FIB can selectively etch one material much faster than surrounding materials, or deposit a metal or oxide. The FIB is used for such tasks as site-specific cross-sectioning for interfacial microstructure studies, preferential removal of certain metals or oxides, semiconductor device editing or modifications, site-specific TEM sample preparation, and grain imaging.

4- Integration of the Research Articles

This Ph.D. thesis work is mainly focused on the preparation, characterization, and biological evaluation (i.e., antibacterial and antibiofilm) of MgF₂ NPs and metal oxides NPs (ZnO, CuO and Zn-CuO). The antibiofilm behavior of all coated teeth was tested against the most popular strain of oral bacteria: *S. mutans*. The work resulted in three publications:

4.1 List of articles:

1. M. Eshed, J. Lellouche, S. Matalon, A. Gedanken, and E. Banin. **Sonochemical Coatings of ZnO and CuO Nanoparticles Inhibit *Streptococcus mutans* Biofilm Formation on Teeth Model.** *Langmuir* 2012, 28, 12288–12295. (Impact factor: 4.187).
2. M. Eshed, J. Lellouche, A. Gedanken, and E. Banin. **A Zn-doped CuO nanocomposite shows enhanced antibiofilm and antibacterial activities against *Streptococcus mutans* compared to nanosized CuO.** *Adv. Funct. Mater.* 2013. (Impact factor: 9.765).
3. M. Eshed, J. Lellouche, A. Gedanken, and E. Banin. **MgF₂ nanoparticle-coated teeth inhibit *Streptococcus mutans* biofilm formation on a tooth model.** *J. Mater. Chem. B* 2013, 1, 3985–3991. (No impact factor yet, being a new journal).

4.2 Integration of the research articles

Our early research focused on the synthesis of ZnO and CuO NPs using ultrasound irradiation, the deposition of the NPs on a teeth model and the examination

of their intrinsic antibacterial properties on *S. mutans* growth. We were surprised to find out that even when the highest concentration of both NPs (1.0 mg/mL) was tested, the growth of *S. mutans* was not affected. Article 1 suggested that the bacteria can induce antioxidant activity to protect itself. To examine this possibility, we tested the activity of major oxidative stress enzymes (superoxide dismutase (SOD) and pseudo-catalase). Thus, our next step was to examine the effects of ZnO and CuO NPs on the formation of *S. mutans* biofilm. And while the ZnO and CuO NPs didn't affect the bacterial growth they had a clear effect on the inhibiting the biofilm formation of *S. mutans*. The objective of article 1 was to present a new method, via ultrasound irradiation, for coating the surface of artificial teeth with ZnO/CuO NPs, and to characterize whether these coated surfaces can restrict bacterial colonization and biofilm formation. We also examined the antibiofilm properties of NP/hydroxyapatite pellets (HA) [129], a major component and an essential ingredient of normal teeth.

Our next step was a sonochemical synthesis of a Zn-doped CuO composite, ($\text{Cu}_{0.88}\text{Zn}_{0.12}\text{O}$, and noted Zn-CuO). The Zn^{+2} ions are doped in the unit cell of the monoclinic CuO lattice replacing the Cu^{+2} ions. The objective of article 2 was a comparison between the antibiofilm and antibacterial activities of Zn-CuO and CuO NPs. As we have shown before, in article 1, CuO and ZnO NPs did not reveal antibacterial activity against *S. mutans* bacteria. In this paper, surprisingly, the Zn-doped CuO composite NPs were found to have some antibacterial activity against *S. mutans* bacteria which finally lead to the enhancement in their antibiofilm activity as well. We further characterized in article 2 the mechanism of antibacterial activity of Zn-CuO nanoparticles. The amounts of Zn^{+2} and Cu^{+2} ions released to an aqueous solution were examined in order to determine whether ions are responsible for the antibacterial activity of the Zn-CuO NPs. Finally the mechanism suggests that the nanoparticles attach to the artificial teeth penetrate into the bacteria, and consequently generate intracellular reactive oxygen species (ROS) which enhance lipid peroxidation and cause cell death.

Article 3 reports on the use of the sonochemistry process to deposit MgF_2 NPs on the surface of artificial teeth and characterized their antibiofilm activity. The originality of Article 3 is the attempt to conduct the experiments as close as possible to real life. Taking in consideration that the tooth paste contains almost always metal fluoride particles. The realization of real life is also reflected in the involvement of

saliva in probing the antibiofilm properties on the MgF₂ NPS. Examining the impact of saliva on this activity provides a proof of concept to our approach. In addition, other new information in the current article is the investigation of the various factors that are responsible for the antibiofilm activity, such as the leaching of F⁻ ions, properties of the coated surface, roughness, and hydrophobicity of the coated surface.

4.3 List of the articles and their abstracts

4.3.1 Article 1

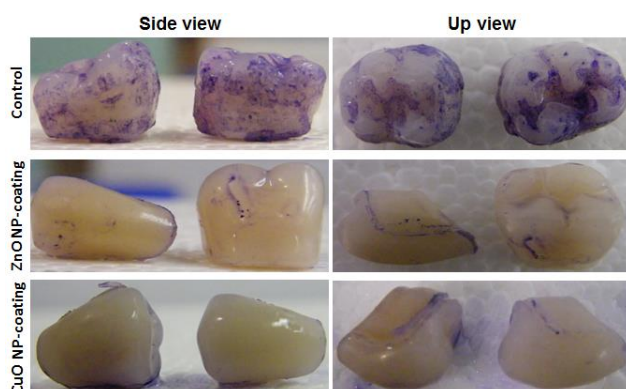
Sonochemical coatings of ZnO and CuO nanoparticles inhibit *Streptococcus mutans* biofilm formation on teeth model

Michal Eshed, Jonathan Lellouche, Shlomo Matalon, Aharon Gedanken,
and Ehud Banin

Langmuir **2012**, 28, 12288–12295

Antibiotic resistance has prompted the search for new agents that can inhibit bacterial growth. We recently reported on the antibiofilm activities of nanosized ZnO and CuO nanoparticles (NPs) synthesized by using sonochemical irradiation. In this study, we examined the antibacterial activity of ZnO and CuO NPs in a powder form and also examined the antibiofilm behavior of teeth surfaces that were coated with ZnO and CuO NPs using sonochemistry. Free ZnO and CuO NPs inhibited biofilm formation of *Streptococcus mutans*. Furthermore, by using the sonochemical procedure, we were able to coat teeth surfaces that inhibited bacterial colonization.

ZnO and CuO NPs-coated teeth restrict *S. mutans* biofilm formation. Coated and uncoated teeth were incubated with *S. mutans* for 24 h. The biofilm biomass that developed was stained by a crystal-violet stain.



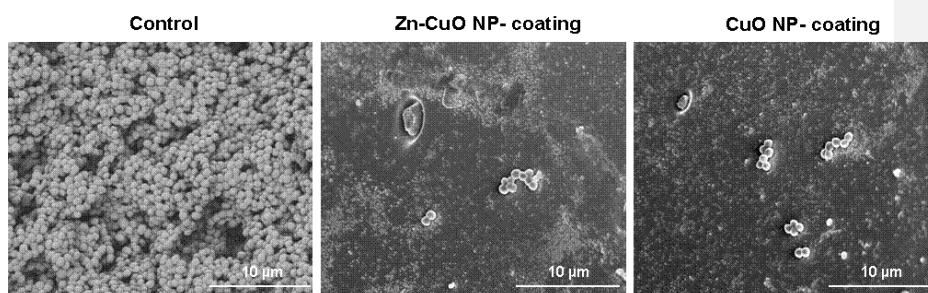
4.3.2 Article 2

A Zn-doped CuO nanocomposite shows enhanced antibiofilm and antibacterial activities against *Streptococcus mutans* compared to nanosized CuO

Michal Eshed, Jonathan Lellouche, Aharon Gedanken, and Ehud Banin

Zinc-doped copper oxide and copper oxide nanoparticles (NPs) were synthesized and deposited on artificial teeth by sonic irradiation, and the ability of these coatings to restrict biofilm formation by *Streptococcus mutans* was examined. The CuO and Zn-CuO NP-coated teeth showed significant reductions in biofilm formation, of 70% and 88%, respectively, compared to uncoated teeth. The mechanism of the Zn-CuO nanoparticles was investigated, revealing that the nanoparticles attach to and penetrate the bacteria and generate intracellular reactive oxygen species (ROS) that enhance lipid peroxidation and cause cell death. Conversely, the CuO or ZnO NPs did not show this behavior and could not generate intracellular ROS. Our results highlight the superior efficacy of Zn-CuO nanocomposites over CuO and ZnO NPs and the role of ROS in their antimicrobial effect.

HR-SEM imaging of *S. mutans* biofilms on coated and uncoated teeth. Biofilms were grown for 24 h at 37°C.



4.3. 3 Article 3

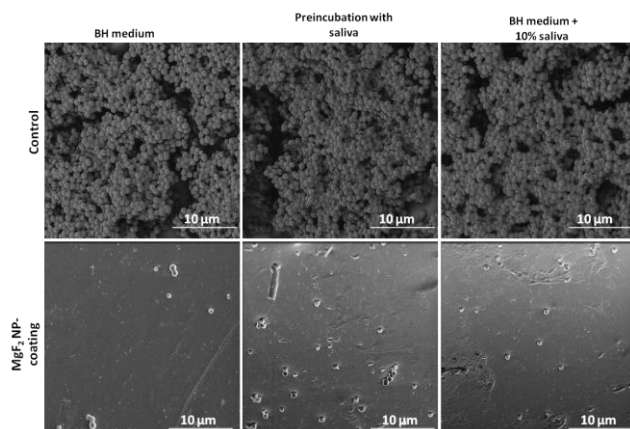
MgF₂ nanoparticle-coated teeth inhibit *Streptococcus mutans* biofilm formation on a tooth model

Michal Eshed, Jonathan Lellouche, Ehud Banin, and Aharon Gedanken

J. Mater. Chem. B, **2013**, *1*, 3985–3991

The formation of biofilms on tooth surfaces, called dental plaque, is a prerequisite for the development of both dental caries and periodontal disease. *Streptococcus mutans* plays an important role in the development of dental caries. Fluoride is routinely used to protect teeth against decay. In the current study, we examined whether we can use a sonochemical based method to coat artificial teeth with MgF₂ nanoparticles (NPs). The results showed that the artificial tooth surface was homogeneously and evenly covered with an MgF₂ NP layer and successful in inhibiting *S. mutans* biofilm formation by over 60%. This antibiofilm activity was also present following incubation with saliva. The activity was dependent on the nano-crystalline characteristics of the material as fluoride ions could induce a similar reduction in biofilm formation. Taken together, our results indicate that the surface modification of artificial teeth with MgF₂ NPs can be effective in preventing the *S. mutans* biofilm.

Teeth surfaces were homogeneously and evenly covered with MgF₂ NP layer. Uncoated control samples supported massive biofilm formation under all tested condition. The coated teeth however, were able to reduce biofilm formation by over 60% compared to the control. No *S. mutans* biofilm formation was observed on NP-coated teeth compared to the uncoated control teeth in which dense colonization was observed. Biofilms were grown for 24 h at 37 °C.



5- Discussion

5.1 Article 1

Sonochemical coatings of ZnO and CuO nanoparticles inhibit *Streptococcus mutans* biofilm formation on teeth model

Michal Eshed, Jonathan Lellouche, Shlomo Matalon, Aharon Gedanken,
and, Ehud Banin

Langmuir **2012**, 28, 12288–12295

The study of *Streptococcus mutans* (*S. mutans*) has been very important in the last years due to their high association with the etiology of dental caries, a biofilm dependent infectious disease. About 95% of populations around the world have been affected by dental caries during their lives; this infectious disease has been a serious health problem for centuries. It is necessary to find an alternative in order to attack this health problem.

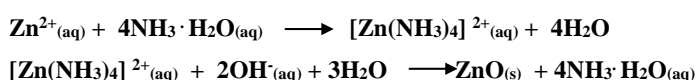
In this paper the preparation of ZnO and CuO NPs using sonochemistry is described. In addition, the aim of this work was to obtain a homogeneous coating of ZnO and CuO NPs on teeth surfaces with a narrow size distribution. This process involves *in situ* generation of ZnO and CuO NPs under ultrasound irradiation and its deposition on teeth in a one-step reaction.

We are aware that the amount of the coated material and their particle size are strongly dependent on the rate of interparticle collisions and on the concentration of the reagents during the sonochemical synthesis. That is why the experimental parameters such as time and concentration of the precursor were selected as important factors for the optimization of the sonochemical reaction.

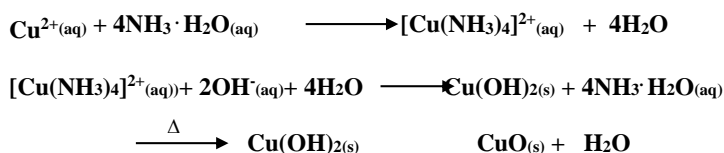
The morphologies of the coated teeth before and after deposition of ZnO and CuO NPs were studied by HRSEM. The sonication reaction created a uniform coating over the entire tooth. The size distribution of ZnO NPs was between 120–180 nm, whereas for CuO NPs the size was 18–20 nm. The topography of the tooth poses a major challenge for coating due to its non-planar surface that contains dents and

protrusions. To examine the coating, elemental mapping analysis was carried out on the top of the tooth and on the wall side of the tooth. The results of these measurements demonstrate a homogeneous coating of teeth with ZnO and CuO NPs.

We considered the coating mechanism as follows: it involves the *in situ* generation of ZnO/ CuONP and their subsequent deposition on teeth in a one-step reaction via ultrasound irradiation. The ZnO is formed during the irradiation according to the following reactions:



The CuO is formed during the irradiation according to the following reactions:



Ammonia works as catalyst for the hydrolysis process, and the formation of ZnO/ CuO takes place through the ammonium complex $[\text{M}(\text{NH}_3)_4]^{2+}$. The metal oxides NPs produced by this reaction are thrown at the surface of the teeth by the sonochemical microjets. These microjets are the after effect of the collapse of sonochemical bubbles.

First, we examined the antibacterial activity of ZnO and CuO NPs towards *S. mutans* and we found that the growth of *S. mutans* was not affected at all. This result is quite surprising since metal oxides are known by their generation of reactive oxygen species (ROS), which were shown as the reason to the antibacterial activity mechanism.

Antibacterial Activity of ZnO NPs- It was found by electron spin resonance (ESR) [130,131] that hydroxyl radicals were present in water suspensions of ZnO. Hydroxyl radical is the most reactive oxygen radical known, and reacts very quickly with almost every type of molecule found in living cells [132]. Such reactions will probably dominate the recombination of two OH radicals to form hydrogen peroxide (H_2O_2). Hydrogen peroxide is also considered to be a weaker oxidizer, but it can cause cell damage via hydroxyl radicals produced by the Fenton reaction [133]. These

results [131] were correlated with the increasing of the antibacterial effect of small NP. Thus, the small size and large specific surface area endow them with high chemical reactivity and intrinsic toxicity. This mode of triggering bacterial cell death can differ for various kinds of bacteria, explicating the difference between *E. coli* and *S. aureus* in the enhancement of the formation of OH radicals [131]. Moreover, *S. aureus* is a more antioxidant protected bacterium, and therefore any burst of free-radical production can be neutralized more easily, ending up, in the short term, with smaller net number of hydroxyl radicals.

Antibacterial Activity of CuO NPs- Following the study of Applerot et al [134], oxy radicals, namely superoxide anions, are generated in CuO water suspensions in addition to the hydroxyl radicals. As usual, the smaller sized particles generating a larger amount of the radicals. Superoxide can act both as a reducing agent, resulting in formation of O_2 , and an oxidizing agent, resulting in formation of hydrogen peroxide.

Schematic illustration of the antibacterial mechanism of CuO NPs [134]:

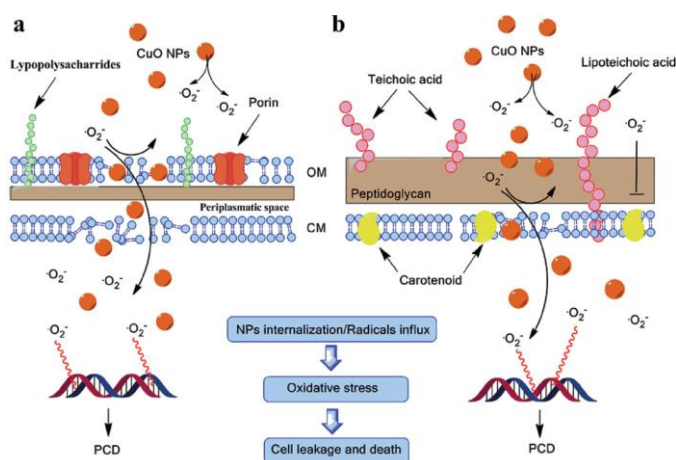


Figure 5.1. Schematic illustration of the antibacterial mechanism of CuO NPs and the relative cellular structure of (a) *E. coli* (Gram-negative) and (b) *S. aureus* (Gram-positive). The major structural differences between the two cells lie in the thickness of the rigid peptidoglycan layer and in the presence of an outer membrane in Gram-negative cells. In Gram-negative cells the peptidoglycan layer is very thin, only a few molecules thick, whereas in Gram-positive cells this layer is very thick. Carotenoid pigments of *S. aureus* provide integrity to its cell membrane and increase its protection

against oxidative stress. The damage to the bacterial cell is mediated by the harmful superoxide anions formed by the cell's attached/internalized CuO NPs.

Previous studies have suggested that ZnO and CuO NPs inhibit *S. mutans* growth [135,136]. One possible explanation for this difference behavior is the possibility that different strains of bacteria were checked in my study and in [135] and [136]. Such a difference can lead to difference in their sensitivity toward oxyradicals. Our hypothesis is that the bacteria can induce antioxidant activity to protect itself. To examine this possibility, we tested the activity of major oxidative stress enzymes (superoxide dismutase (SOD) and pseudo-catalase).

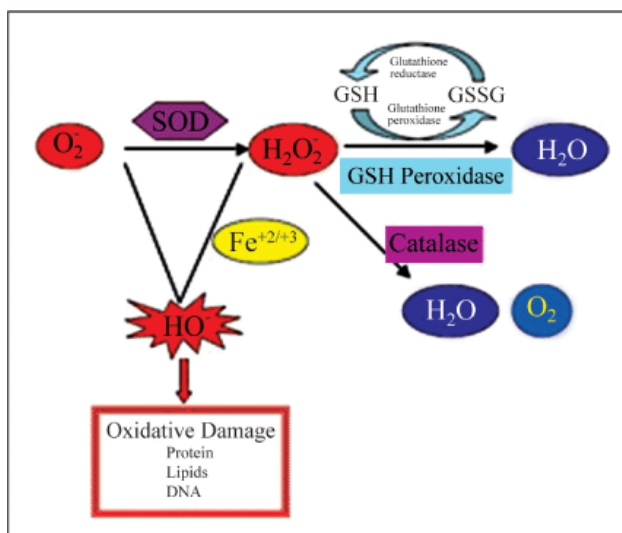


Figure 5.2. Defense mechanism against damage by ROS. Superoxide dismutase (SOD) plus catalase or glutathione peroxidase (GPx) eliminate many damaging oxygen species.

The effects of these reactive species are wide-ranging, but three reactions are particularly relevant to cell injury: lipid peroxidation of membranes, oxidative modification of proteins, oxidative damages to DNA. Cells have defense systems to prevent injury caused by ROS. The toxic effect of these reactive oxygen species and free radicals can be eliminated by enzymes such as superoxide dismutase (SOD), one of the main antioxidant systems which eliminates O_2^- to produce H_2O_2 [137]. The H_2O_2 is eliminated by glutathione peroxidase or by catalase. We have shown that SOD

and pseudo-catalase activities in *S. mutans* are slightly increased upon exposure to the NPs as compared to the control. In other words, as a line of defense against oxidative stress and cytoplasmic ROS, the antioxidant enzymes activities increased upon NPs exposition. This result may explain the increased resistance of the planktonic cultures to the oxidative stress. As mentioned above although no antibacterial activity of the NPs was observed, clear antibiofilm of these NPs was detected. . We examined the antibiofilm properties on the following surfaces:

1. Artificial teeth
2. Hydroxyapatite (HA) pellets with NPs

Since up to 50% (wt.) of the bone is a modified form of hydroxylapatite (known as bone mineral) and carbonated calcium-deficient hydroxylapatite is the main mineral of which dental enamel and dentin are composed. HA is known to be considered for tooth or bone replacement and a model for tooth surface [129]. We have checked whether we can probe its antibiofilm activity thus highlighting the possibility for future application. We evaluated the antibiofilm activity of the mixture NP/hydroxyapatite using two biofilm models (static and dynamic, continuous culture flow).

The ZnO and CuO NP-coated teeth show significant reduction in biofilm formation by 85% and 70%, respectively. The pellets that contain NPs, NP/hydroxyapatite, are able to completely inhibit *S. mutans* biofilm formation.

5.2 Article 2

Zn-doped CuO nanocomposite show enhanced antibiofilm and antibacterial activities against *Streptococcus mutans* compared to nanosized CuO

Michal Eshed, Jonathan Lellouche, Aharon Gedanken, and Ehud Banin

In the current paper, we describe a comparison study between CuO NPs and Zinc-doped copper oxide (Zn-CuO) NPs towards their antibacterial and antibiofilm

properties against *S. mutans*. In other words, the objective of the current study was to present the differences in the antibiofilm and antibacterial activities of Zn-CuO and CuO NPs.

For the antibiofilm study, Zinc-doped copper oxide and copper oxide nanoparticles. Both NPs were synthesized and deposited on artificial teeth by using sonochemical irradiation. HR-SEM, RBS and FIB-SEM techniques were used to examine the coated layers on the tooth surface. Next we examined the ability of teeth surfaces that were coated with Zn-CuO and CuO NPs to restrict biofilm formation of *S. mutans*. Both the CuO and Zn-CuO NP-coated teeth show significant reduction in biofilm formation by 70% and 88%, respectively, compared to uncoated tooth. In this paper, surprisingly, the Zn-doped CuO composite NPs were found to have some antibacterial activity against *S. mutans* bacteria which finally lead to enhancement in its antibiofilm activity as well. Based on the antibacterial results we continued to address the mechanism of action of the Zn-CuO NPs. The mechanism of the antibacterial activity of metal oxides is poorly understood, and still under controversy in the literature. Suggested mechanisms include: 1- the role of reactive oxygen species (ROS) generated on the surface of the particles, 2 - ion release, 3 - membrane dysfunction, and 4- nanoparticle internalization.

Liberation of metal ions: It is well known that metallic ions, such as silver [138], copper [139], and zinc [136], have strong inhibitory and bactericidal effects on a broad spectrum of bacteria. The cytotoxicity of NP-generated ions is due to the interaction between ions and thiol groups in proteins or enzymes in microorganisms which leads to the inhibition of their crucial biological functions [137]. Cu^{+2} ions are a potent inhibitor of several enzymes and metabolic pathways in the bacterial cell [138]. The Cu^{+2} ions can combine with the membrane by electrostatic attraction and penetrate into the cell membrane through membrane channels. Once inside the cell, Cu^{+2} can strongly combine with intracellular sulfur-containing amino acids, which lead to denaturation of proteins and can result in cell death. In fact, several studies have demonstrated the efficacy of copper ions to reduce plaque formation in humans and to inhibit its ability to generate acid after exposure to sucrose [139-141]. The antimicrobial activity was attributed to Cu^{+2} oxidizing key thiol groups in bacterial metabolic enzymes [142]. According to the literature [139,143], when 1 mmol/L

Cu⁺² was provided in the drinking water, rats infected with *S. mutans* had significantly reduced experimental caries and significantly reduced populations of *S. mutans* colonizing the tooth surface. It was also found that in the case of Zn⁺² ions, the higher content of Zn⁺² have a pronounced effect against pathogens [144]. Additionally, the effects of metal ions such as Zn⁺² and Cu⁺² on glucosyltransferases were also reported [145]. Glucosyltransferase activity mediates sucrose-dependent adherence of *S. mutans* to the tooth surface, this is essential for the cariogenicity of these microorganisms, and contributes significantly to the exopolysaccharide component of the dental-plaque matrix. The cationic metals Zn⁺² and Cu⁺² were found to produce significant inhibition of glucosyltransferases. From the above it is clear that Cu⁺² and Zn⁺² appears to have an effect on cariogenic bacteria colonizing tooth surface and that the mechanism of action could be attributed to inhibition of bacterial metabolism and subsequent bacterial growth. Our aim now was to examine two metal cations: Cu⁺² and Zn⁺² for their ability to act as inhibitors of *S. mutans* growth. To begin and address this we first measured the concentrations of Zn⁺² and Cu⁺² ions, which have been released from Zn-CuO and CuO NPs (1 mg/mL) in BH medium after a period of 24 hours. The results indicate that Cu⁺² and Zn⁺² ions have no effect on the antibacterial activity.

NP internalization: This is another important factor that influences the biocidal activity of metal oxides nanostructures. The detailed mechanism by which the nanostructures with smaller size can penetrate through some damaged areas of the bacterial membrane remains to be determined. Surface charge has a significant impact on particle internalization [146]; the primary interaction of the nanostructure with the bacteria is probably via an electrostatic attraction between the nanostructure surface and positively charged regions of the extracellular domain of integral membrane proteins on the cell surface [146]. After the internalization occurs, the internalized nanostructures may follow multiple pathways into the cell [146]; the internalization kinetics appears to be interdependent on the effective ratio, absolute size and volume of nanostructure [146].

Studies of MgF₂ [147], ZnO [148], and CuO [149] NPs have observed the presence of NPs in the cytoplasm of damaged cells and the inferred transport of particles across both the outer and inner membranes. One possible route for NP

ingress is via various pores in the outer membrane. The largest pores in the bacterial outer membrane are probably those used to secrete mature proteins, either onto the outer membrane surface or into the wider milieu. For example, the secretin family of proteins is associated with the outer membrane of various Gram-negative bacteria, forming ring-shaped pore structures [150]. In *P. aeruginosa*, elastase is secreted in its folded form with a maximum width of 6 nm via secretin [151]. Such pores are theoretically large enough to allow the passage of 1-9 nm NPs. However, due to its large size, the pore is probably gated (closed) to prevent loss of cytoplasm. Effectively, the channel is only open when it is required to transport proteins across the outer membrane [150]. Thus, it is likely that NPs are prevented from crossing even the largest of outer membrane pores. The observation of NPs in the cytoplasm most probably arises from Brownian diffusion after the membrane is disrupted [146].

In summary, the death of bacteria in the presence of various NPs appears to be due to membrane disruption. Close contact is necessary for membrane disruption to occur, and it is unlikely that NPs cross into the cytoplasm until the membranes become sufficiently porous.

In a further effort to understand the antibacterial activity of Zn-CuO particles as compared to CuO particles we also utilized TEM measurements to examine the effect of nanoparticles on the bacteria. Zn-CuO NPs with *S. mutans* cells show that the nanoparticles are localized either on the cell surface or within the cell membrane. Moreover, in the case of Zn-CuO NPs, the cell membrane looks damaged and disorganized, while in the case of CuO NPs, the cell membrane remains intact, without visible injuries.

Zeta potential and antibacterial activity: Zeta potential plays a significant role in a particle's ability to penetrate into cell bodies. To the extent that ROS may be involved in NP toxicity, which is mainly mediated by surface charges, direct contact between NPs and the bacterial membrane appears essential [152,153]. The charges which develop at the interface between a particle (or a bacteria cell) and the surrounding medium may arise from the dissociation of ionogenic groups at the particle surface and from the differential adsorption of solution ions possessing different charges.

The fact that Zn-CuO nanoparticles were observed at the surface of cell membranes may be related to the zeta potential that is known to affect

the antimicrobial activity [56]. The zeta potential measurements revealed that the average charges of Zn-CuO NPs and CuO NPs are -12 mV and -13.9 mV, respectively. Although strongly positive zeta potential of a nanoparticle promotes its interactions with cell membranes, Zn-CuO NPs which have a negative zeta potential can still promote interaction with cell membrane and even have the ability to penetrate into the bacteria's cells. The negative zeta potential of the nanoparticles, and minimal electrostatic interactions with the negative charge on the bacteria surface, may explain why relatively high concentrations of nanoparticles were needed to produce an antibacterial effect.

Intracellular ROS Concentration: Intracellular ROS could be easily measured by using fluorescein diacetate-derived fluorescent probes. The cell-permeable probe is deacetylated by intracellular esterases to activate the probe, which is readily oxidized by ROS, forming a highly fluorescent probe. We have shown that the exposure of *S. mutans* to Zn-CuO NPs induced intracellular oxidative stress and the cytoplasmic concentration of ROS increased dramatically after an NP-exposure.

NP-bacterial membrane lipid peroxidation: Fundamental insight into the interaction of NPs with bacterial cell membranes would provide direction in the design of bactericidal agents. However, the interaction of NPs with bacterial cell membranes is not well understood. No good models concerning how this interaction takes place or the loci to which the NPs are most attracted have been proposed. Depending upon the specific membrane and the NP structure, membrane interactions with nanoparticles matter can result in blebbing, tubule formation, or the creation or enlargement of membrane defects, etc., in a subtle structural interplay of the NP and membrane structures.

Metal NPs appear to disrupt important membrane activities and are therefore considered damaging rather than toxic. The mechanisms by which membranes become compromised in the presence of metal oxides NPs are currently thought to involve lipid peroxidation by reactive oxygen species such as superoxide ions (O_2^-) and hydroxyl radicals ($\bullet OH$) [154]. Lipid peroxidation is a signature of ROS damage. Lipids containing polyunsaturated fatty acids are susceptible to free radical-initiated oxidation and can participate in chain reactions that increase damage to

biomolecules[155]. Lipid peroxidation, which leads to lipid hydroperoxide formation often, occurs in response to oxidative stress.

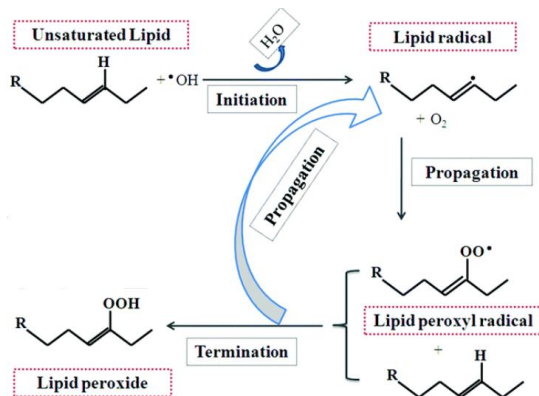


Figure 5.3. Mechanism of lipid peroxidation. This process proceeds by a free radical chain reaction mechanism. It most often affects polyunsaturated fatty acids, because they contain multiple double bonds in between which lie methylene $-\text{CH}_2-$ groups that possess especially reactive hydrogen. As with any radical reaction, the reaction consists of three major steps: initiation, propagation, and termination.

To determine the effect of Zn-CuO NPs and CuO NPs on membrane lipid peroxidation, we followed malondialdehyde (MDA) production (as a marker for lipid peroxidation) in *S. mutans*. We have found that addition of the Zn-CuO NPs increased the concentration of MDA detected in the cells more than in the case of addition of CuO NPs in the same concentrations.

Taken together, the ability of many of the metal NPs to generate ROS and their direct contact with the cells is considered to be the major mechanism by which these NPs exhibit their toxic effects [156-158]. Hence, we propose that there are two essential requirements: first, strong adherence of the particles to the bacterial cell membrane, as could have been seen only in the case of Zn-CuO NPs and second, ROS generation that damages the cells.

5.3 Article 3

MgF₂ nanoparticle-coated teeth inhibit *Streptococcus mutans* biofilm formation on a tooth model

Michal Eshed, Jonathan Lellouche, Ehud Banin, and Aharon Gedanken

The objective of the current study was to evaluate the use of ultrasound irradiation, for coating the surface of artificial teeth with MgF₂ NPs and its impact on *S. mutans* biofilm formation.

HR-SEM on the tooth surface and on the area of groove and pit in the tooth shows that MgF₂ NPs form a uniform layer of spherical NPs with an average size of 48 nm. One of the factors influencing the applicability of our approach is the release of NPs into the surrounding environment. We have carried out the leaching experiments in BH medium and to pure saliva (without bacteria) for 24 hours. No MgF₂ NPs were detected, indicating no leaching of NPs from the teeth surface. Moreover, leaching was also measured after brushing the tooth. Again, no MgF₂ NPs were detected. This indicates that a strong attachment of the NPs to the tooth is obtained when they are deposited sonochemically.

The originality of the current manuscript is the attempt to conduct the experiments as close as possible to real life. This is reflected first in the use of a metal fluoride. Metal fluoride particles are a component of almost all tooth pastes. In addition what brings my project to real life is the involvements of saliva in probing the antibiofilm properties on the MgF₂ NPs. Saliva components have the following function, and mostly dual role:

Table 5.1. Various components of saliva and their functions:

Function	Salivary component
Antibacterial Agents	Histatins, IgA, IgM, Lactoferrin, Lactoperoxidase, Lysozyme, Mucins, Proline- rich proteins, Statherin
Inhibitors of microbial adherence	IgA, IgM
Participate in oral bacterial adhesion to human host cells	IgA, Mucins, Proline- rich proteins, Amylase, Fibronectin, Statherin, Lysozyme, Lactoferrin

For example, fibronectin [159], which is a glycoprotein that is present in many body fluids and tissues as well as in saliva, induces bacterial aggregation by its ability to bind to buccal epithelial cells and serves as a major receptor for Group A *Streptococci*,

but it inhibits the adherence of several gram-negative species such as *Escherichia coli* [160-162].

In order to check whether a surface covered with MgF₂ NPs can overcome the presence of proteins that contribute and encourage *S. mutans* biofilm formation, we divided the teeth into three groups. (i) Teeth with *S. mutans* bacteria immersed in BH medium (ii) Teeth that were incubated for 1 hour in saliva, washed and then immersed in BH medium (iii) Teeth with *S. mutans* bacteria immersed in BH medium that contains 10% saliva. In each group we compared the behavior of uncoated teeth against teeth which were coated with MgF₂ NPs. The coated teeth, however, were able to reduce biofilm formation by over 60% compared to the control in all three experimental conditions. A major question is whether the observed antibiofilm activity is associated with the levels of the F⁻ anions or the activity requires the crystalline nano-structure of the MgF₂ nanoparticle. The fluoride anion has known antibacterial activities [163]. F⁻ anion concentration was measured after exposing the coated tooth to BH medium for 24 hours, in order to evaluate the effects of fluoride anion on *S. mutans* biofilm formation. The results indicate that fluoride anion was only able to reduce biofilm formation by 9%. This result indicates that other unique mechanisms may govern the antibiofilm properties of the surfaces. This result further substantiates our hypothesis that the nano crystalline nature of the MgF₂ NPs is crucial for the observed antibiofilm activity. Our results indicate that the surface modification of artificial teeth with MgF₂ NPs can be effective in preventing *S. mutans* biofilm.

Nanoscale materials provide roughness and dimensions at the nano level which might influence bacteria behavior. It was also demonstrated that the attachment of different pathogenic strains (*S. aureus*, *S. epidermidis*, and *P. aeruginosa*) could be controlled by changing titanium surface roughness and ultrafine crystallinity at the nano level [164].

Roughness in the contact of biofilm can be divided into two categories (Figure 5.4) [56]:

1. Micronscale roughness: has been identified as an undesirable property in biomaterial surfaces due to the bacteria's ability to more easily establish the biofilm in grooves or pits on the material surface.

2. Nanorough surfaces: were found to reduce the adhesion of bacteria by preventing close contact of the cell wall to the material surface due to the relative rigidity of the cell wall [56]. In contrast to a eukaryotic cell, which is very flexible a bacteria cell wall may be unable to conform to the topography of a material with nanoscale surface features, inhibiting the early stages of bacteria adhesion. Nanoscale features might inhibit the electrostatic interactions responsible for initial bacterial attachment on the surface [165]. Accumulation of proteins on nanorough surfaces might also affect initial bacterial adhesion through a thick protein layer [166]. This layer could decrease interactions at the bacteria–nanorough surface interface. Thus, this passivation effect could reduce bacterial attachment and biofilm formation [166].

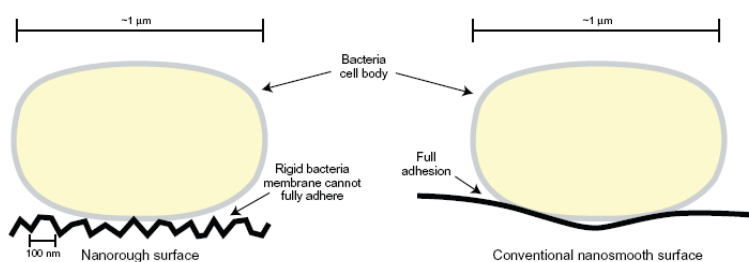


Figure 5.4. Illustration comparing bacteria surface interactions with nanorough surfaces and conventional nanosmooth surfaces. Due to the high degree of roughness on nanomaterials, rigid bacteria cell membranes cannot lay flush against the material surface. This may inhibit the preliminary steps which lead to bacteria adhesion. As a result, bacteria activity on a nanomaterial surface may be reduced.

The surface coated by MgF₂ NPs has a higher roughness, 5 times more than surface without particles. This study indicated that there is a great potential to create anti biofilm surfaces via engineering surface roughness at the nanoscale.

Surface nanoroughness can provide more surface area and make the surface more hydrophobic. Hydrophobicity of teeth surfaces were characterized by contact angle measurements. Coated tooth with MgF₂ NPs were more hydrophobic than the control. It has been found that adhesion of bacteria to materials is controlled by the degrees of hydrophobicity of both bacteria and material surface [167,168]. Furthermore, the formation of dental plaque on surfaces in the human oral cavity is far less abundant on

hydrophobic than on hydrophilic surfaces [169]. According to interfacial thermodynamics, bacteria that pose a high surface free energy, such as *S. mutans*, should adhere preferentially to a hydrophilic substrate [170,171]. It may be hypothesized that the decrease in initial adhesion of *S. mutans* to the tooth surface upon the presence of MgF₂ NPs was due to the latter's significantly increased hydrophobicity.

5.4 Conclusions

Nanoparticles with intrinsic anti biofilm properties (ZnO, CuO, Zn-CuO and MgF₂) can be synthesized and uniformly deposited onto the surface artificial teeth by the sonochemical method. The coating was performed by a simple, efficient, one-step procedure using environmentally friendly reagents. The physical and chemical analyses demonstrated that nanoparticles are finely dispersed onto the teeth surfaces. The coated teeth with these different NPs were successful in inhibiting *S. mutans* biofilm formation even in the presence of saliva (in the case with MgF₂). This dissertation addresses the issues which appear critical in determining the anti biofilm and antibacterial activities. As we have shown, surface chemistry and topography, including nanoscale topography and hydrophobicity, have been extensively studied in relation to bacteria's adhesion. Of all the NPs that were investigated in this study, only one was discovered to have antibacterial activity against *S. mutans* bacteria. However, all four NPs revealed inhibition of the growth of biofilm. The antibacterial mechanism of these nanoparticles was investigated. Taken together, our study further highlights the potential of the different NPs that were investigated in this research, to inhibit biofilm formation in the context of the oral niche.

6 - References

1. Cao, G. *Nanostructures and Nanomaterials*, World Scientific Publishing, Singapore, **2004**, p.3
2. Carreon, M.A.; Guliants, V.V. *Eur. J. Inorg. Chem.* **2005**, *1*, 27.
3. Gedanken, A. *Ultrasonics Sonochemistry* **2004**, *11*, 47.
4. Perelshtein, I.; Applerot, G.; Perkas, N.; Grinblat, J.; Gedanken, A. *Chemistry-A European Journal* **2012**, *18*, 4575.
5. Applerot, G.; Lellouche, J.; Perkas, N.; Nitzan, Y.; Gedanken, A.; Banin, E. *RSC Advances* **2012**, *2*, 2314.
6. Gottesman, R.; Shukla, S.; Perkas, N.; Solovyov, L.A.; Nitzan, Y.; Gedanken, A. *Langmuir* **2011**, *27*, 10340.
7. Mertl, M. *AAAS Meeting :Neurobiol. Sci.* **1999**, *283*, 775.
8. Niu, H.; Chen, Q.; Zhu, H.; Lin, Y.; Zhang, X. *J. Mater. Chem.* **2003**, *13*, 1803.
9. Stoodley, P.; Sauer, K.; Davies, D. G.; Costerton, J. W. *Annual Reviews in Microbiology* **2002**, *56*, 187.
10. Parsek, M. R.; Singh, P. K. *Annual Reviews in Microbiology* **2003**, *57*, 677.
11. **Biofilm hypertextbook, Montana State University Center for Biofilm Engineering.**
12. Marsh, P.D. *Journal of Dentistry* **2010**, *38*, S11.
13. Newman, B. M.; White, P.; S. Mohan, B.; Cole, J. A. *J. Gen. Microbiol.* **1980**, *118*, 353.
14. Saxton, C. A. *Arch. Oral Biol.* **1969**, *14*, 1275.
15. Rogers, A. H. *Arch. Oral Biol.* **1976**, *21*, 99.
16. Marsh, P. D.; Moter, A.; Devine, D. A. *Periodontology 2000* **2011**, *55*, 16.
17. Marsh, P. D.; Martin, M. V. *Oral Microbiology*, 5th ed. Edinburgh: Churchill LivingstoneElsevier **2009**.
18. Jakubovics, N. S. *Molecular Oral Microbiology* **2010**, *25*, 4.
19. Philip D. Marsh, P. D. *Compendium* **2009**, *30*, 76.
20. Allison, D. G.; Gilbert, P.; Lappin- Scott, H. M. *Community Structure and Co-operation in Biofilm*. 1 st ed. Cambridge, United Kingdom: Cambridge University Press **2000**, 65.
21. Yang, L.; Liu, Y.; Wu, H.; Song, Z.; Hoiby, N.; Molin, S.; Givskov, M. *Fems Immunology and Medical Microbiology* **2012**, *65*, 146.
22. Redelman, C. V.; Hawkins, M. A. W.; Drumwright, F. R.; Ransdell, B.; Marrs, K.; Anderson, G. G. *Biochemistry and Molecular Biology Education* **2012**, *40*, 191.
23. Hoiby, N.; Bjarnsholt, T.; Givskov, M.; Molin, S.; Ciofu, O. *International Journal of Antimicrobial Agents* **2010**, *35*, 322.
24. Stewart, P. S. *Antimicrobial Agents and Chemotherapy* **1996**, *40*, 2517.
25. Stewart, P. S.; Franklin, M. J. *Nature Reviews Microbiology* **2008**, *6*, 199.
26. Brown, M. R. W.; Allison, D. G.; Gilbert, P. *Journal of Antimicrobial Chemotherapy* **2005**, *22*, 777.
27. Poole, K. *Trends in Microbiology* **2012**, *20*, 227.
28. Adnan, M.; Morton, G.; Singh, J.; Hadi, S. *Molecular and Cellular Biochemistry* **2010**, *342*, 207.

29. Ritter, A.; Com, E.; Bazire, A.; Goncalves, M. D. S.; Delage, L.; Le Penne, G.; Pineau, C.; Dreanno, C.; Compere, C.; Dufour, A. *Proteomics***2012**, *12*, 3180.
30. Toyofuku, M.; Roschitzki, B.; Riedel, K.; Eberl, L. *Journal of Proteome Research***2012**, *11*, 4906.
31. Kuchma, S. L.; O'Toole, G. A. *Current Opinion in Biotechnology***2000**, *11*, 429.
32. Maira-Litran, T.; Allison, D. G.; Gilbert, P. *Journal of Antimicrobial Chemotherapy***2000**, *45*, 789.
33. Brooun, A.; Liu, S. H.; Lewis, K. *Antimicrobial Agents and Chemotherapy***2000**, *44*, 640.
34. Stewart, P. S.; Costerton, J. W. *Lancet***2001**, *358*, 135.
35. Mah, T. F. C.; O'Toole, G. A. *Trends in Microbiology***2001**, *9*, 34.
36. Selwitz, R. H.; Ismail, A.; Pitts, N. B. *Lancet***2007**, *369*, 51.
37. Featherstone, J. D. *Community Dent Oral Epidemiol.* **1999**, *27*, 31.
38. Featherstone, J. D. *Pediatr Dent.***2006**, *28*, 128.
39. Featherstone, J. D. *JADA***2000**, *131*, 887.
40. Featherstone JD. Caries prevention and reversal based on the caries balance. *Pediatr Dent* 2006;*28*(2):128-132; discussion 192-198. כמו רפרנס 35
41. Marsh PD, Martin MV. *Oral Microbiology*, 5th edn. Edinburgh: Churchill Livingstone; 2009. רפרנס 14
42. Marsh, P. D. *Microbiology***2003**, *149*, 279.
43. Becker, M. R.; Paster, B. J.; Leys, E. J.; Moeschberger, M. L.; Kenyon, S. G.; Galvin, J. L.; Boches, S. K.; Dewhirst, F. E.; Griffen, A. L. *J. Clin. Microbiol.* **2002**, *40*, 1001.
44. Bowden, G. H. *J. Dent. Res.***1990**, *69*, 1205.
45. Bowden, G. H.; Hardie, J. M.; McKee, A. S.; Marsh, P. D.; Fillery, E. D.; Slack, G. L. The microflora associated with developing carious lesions of the distal surfaces of the upper first premolars in 13–14 year old children. In *Proceedings Microbial Aspects of Dental Caries Volume 1*. Edited by: Stiles HM, Loesche WJ, O'Brien TC. Washington DC: Information Retrieval Inc.; 1976:233-241.
46. Marsh, P. D. *J. Dent. Res.***1989**, *68*, 1567.
47. Marsh, P. D. *Dent. Clin. North. Amer.***1999**, *43*, 599.
48. Socransky, S.S.; Haffajee, A.D. *Periodontology 2000***2005**, *38*, 135.
49. Loesche, W. J. *Microbiol Rev.***1986**, *50*, 353.
50. Newbrun, E. *Sp Suppl Microbiology Abstracts* **1974**, *111*, 655.
51. Carlsson, J.; Hamilton, I. R. *Metabolic Activity of Oral Bacteria*, 2nd edn. Copenhagen: Munksgaard. **1994**.
52. Ahn, S. J.; Wen, Z. T.; Burne, R. A. *Infect Immun.***2006**, *74*, 1631.
53. Jordan, S.; Junker, A.; Helmann, J. D.; Mascher, T. J. *Bacteriol.***2006**, *188*, 5153.
54. Banerjee, I.; Pangule, R. C.; Kane, R. S. *Adv. Mater.***2011**, *23*, 690.
55. Kwaadsteniet, D. M.; Botes, M.; Cloete, T. E. *Nano***2011**, *6*, 395.
56. Darouiche, R. *International Journal of Artificial Organs***2007**, *30*, 820.
57. Zitzmann, N. U.; Berglundh, T. J. *Clin. Periodontol.* **2008**, *38*, 286S.
58. Yacoby, I.; Benhar, I. *Nanomedicine***2008**, *3*, 329.
59. Seil, J. T.; Webster, T. J. *International Journal of Nanomedicine***2012**, *7*, 2767.
60. Allaker, R.P. *J. Dent. Res.***2010**, *89*, 1175.
61. Stewart, P. S. *J. Bacteriol.* **2003**, *185*, 1485.

62. Wilson, M.J. *Med. Microbiol.* **1996**, *44*, 79.
63. Baehni, P. C.; Takeuchi, Y. *Oral Dis.* **2003**, *9*, 23.
64. Watson, P. S.; Pontefract, H. A.; Devine, D. A.; Shore, R. C.; Nattress, B. R.; Kirkham, J.; Robinson, C. *J. Dent. Res.* **2005**, *84*, 451.
65. Wood, S. R.; Kirkham, J.; Marsh, P. D.; Shore, R. C.; Nattress, B.; Robinson, C. *J. Dent. Res.* **2000**, *79*, 21.
66. Nel, A. E.; Madler, L.; Velegol, D.; Xia, T.; Hoek, E. M.; Somasundaran, P.; Klaessig, F.; Castranova, V.; Thompson, M. *Nat. Mater.* **2009**, *8*, 543.
67. Cao, H.; Suib, S. L. *J. Am. Chem. Soc.* **1994**, *116*, 5334.
68. Ao, R.; Kummerl, L.; Haarer, D. *Adv. Mater.* **1995**, *7*, 495.
69. Andrew, L. *Ecotoxicology* **2008**, *17*, 362.
70. Hess, H.; Tseng, Y. *ACS Nano* **2007**, 1390.
71. Anagnostakos, K.; Hitzler, P.; Pape, D.; Kohn, D.; Kelm, J. *Acta Orthop.* **2008**, *79*, 302.
72. Stoimenov, P. K.; Klinger, R. L.; Marchin, G. L.; Klabunde, K. J. *Langmuir* **2002**, *18*, 6679.
73. Chopra, K.L.; Das, S.R. (Eds.), *Thin Film Solar Cells*, Plenum, New York, **1983**.
74. Larcheri, S.; Armellini, C.; Rocca, F.; Kuzmin, A.; Kalendarev, R.; Dalba, G.; Graziola, R.; Purans, J.; Pailharey, D.; Jandar, F. *Superlattices Microst.* **2006**, *39*, 267.
75. Wang, Z.L.; Phys, J. *Condens. Matter.* **2004**, *16*, 829.
76. Look, D.C.; Claflin, B. *Phys. Stat. Sol.* **2004**, *241*, 624.
77. Stoimenov, P. K.; Klinger, R. L.; Marchin, G. L.; Klabunde, K. J. *Langmuir* **2002**, *18*, 6679–6686. **כמו רפרנס 69**
78. Axtell, H. C.; Hartley, S. M.; Sallavanti, R. A. U.S. Patent 5,026,778, **2005**.
79. Premanathan, M.; Karthikeyan, K.; Jeyasubramanian, K.; Manivannan, G. *Nanomed. Nanotechnol. Biol. Med.* **2011**, *7*, 184.
80. Sivakumar, P. M.; Balaji, S.; Prabhawathi, V.; Neelakandan, R. *Carbohydr. Polym.* **2010**, *79*, 717.
81. Ma, X.; Zhang, W. *Polym. Degrad. Stab.* **2009**, *94*, 1103.
82. Sderberg, T. A.; Sunzel, B.; Holm, S.; Elmros, T.; Hallmans, G.; Sjoberg, S. *Scand J. Plast. Reconstr. Surg. Hand. Surg.* **1990**, *24*, 193.
83. Fang, M.; Chen, J. H.; Xu, X. L.; Yang, P. H.; Hildebrand, H. F. *Inter. J. Antimicrob. Agents* **2006**, *27*, 513.
84. Adams, L. K.; Lyon, D. Y.; McIntosh, A.; Alvarez, P. J. *Water Sci. Technol.* **2006**, *54*, 327.
85. Jones, N.; Ray, B.; Ranjit, K. D.; Manna, A. C. *FEMS. Microbiol. Lett.* **2008**, *279*, 71.
86. Applerot, G.; Lipovsky, A.; Dror, R.; Perkas, N.; Nitzan, Y.; Lubart, R.; Gedanken, A. *Adv. Funct. Mater.* **2009**, *19*, 842.
87. Singh, D. P.; Ali, N. *Sci. Adv. Mat.* **2010**, *2*, 295.
88. Kasemets, K.; Ivask, A.; Dubourguier, H. C.; Kahru, A. *Toxicol. In Vitro* **2009**, *23*, 1116.
89. Anyaogu, K. C.; Fedorov, A. V.; Neckers, D. C. *Langmuir* **2008**, *24*, 4340.
90. Borkow, G.; Zhou, S. S.; Page, T.; Gabbay, J. A. *PLoS One* **2010**, e11295.
91. Cox, C. *J. Pestic. Reform* **1991**, *11*, 2.
92. Gabbay, J.; Borkow, G.; Mishal, J.; Magen, E.; Zatcoff, R.; Shemer-Avni, Y. *J. Ind. Text.* **2006**, *35*, 323.

93. Paschoalino, M.; Guedes, N. C.; Jardim, W.; Mielczarski, E.; Mielczarski, J. A.; Bowen, P.; Kiwi, J. *J. Photochem. Photobiol. A: Chem.* **2008**, *199*, 105.
94. Xia, T.; Kovochich, M.; Liong, M.; Mädler, L.; Gilbert, B.; Shi, H.; Yeh, J. I.; Zink, J. I.; Nel, A. E. *ACS. Nano* **2008**, *2*, 2121.
95. Gunawan, C.; Teoh, W. Y.; Marquis, C. P.; Lifia, J.; Amal, R. *Small* **2009**, *5*, 341.
96. Limbach, L. K.; Wick, P.; Manser, P.; Grass, R. N.; Bruinink, A.; Stark, W. J. *Environ. Sci. Technol.* **2007**, *41*, 4158.
97. Islam, B.; Khan, S. N.; Khan, A. U. *Med. Sci. Monit.* **2007**, *13*, RA196.
98. Frazier, P. D.; Little, M. F.; Casciani, F. S. *Arch. Oral. Biol.* **1967**, *12*, 35.
99. Brown, W. E.; Gregory, T. M.; Chow, L. C. *Caries Res.* **1977**, *11*, 118.
100. Johnston, D. W. *Community Dent. Oral. Epidemiol.* **1994**, *22*, 159.
101. Featherstone, J. D. *Community Dent. Oral Epidemiol.* **1999**, *27*, 31.
102. Neri, F.; Kok, D.; Miller, M. A.; Smulevich, G. *Biochemistry* **1997**, *36*, 8947.
103. Bunick, F. J.; Kashket, S. *Infection and Immunity* **1981**, *34*, 856.
104. Phan, T. N.; Kirsch, A. M.; Marquis, R. E. *Oral Microbiology and Immunology* **2001**, *16*, 28.
105. Sternweis, P. C.; Gilman, A. G. Aluminum - a requirement for activation of the regulatory component of adenylate-cyclase by fluoride. Proceedings of the National Academy of Sciences of the United States of America-Biological Sciences. 1982;79:4888-91.
106. Petsko, G. A. *Proc. Natl. Acad. Sci. USA.* **2000**, *97*, 538.
107. Miles, R. D.; Gorrell, A.; Ferry, J. G. *Journal of Biological Chemistry* **2002**, *277*, 22547.
108. Datta, S.; Prabu, M. M.; Vaze, M. B.; Ganesh, N.; Chandra, N. R.; Muniyappa, K.; Vijayan, M. *Nucleic Acids Res.* **2000**, *28*, 4964.
109. Cho, H. S.; Lee, S. Y.; Yan, D. L.; Pan, X. Y.; Parkinson, J. S.; Kustu, S.; Wemmer, D. G.; Pelton, J. G. *Journal of Molecular Biology* **2000**, *297*, 543.
110. Yan, D.; Cho, H. S.; Hastings, C. A.; Igo, M. M.; Lee, S. Y.; Pelton, J. G.; Stewart, V.; Wemmer, D. E.; Kustu, S. *Proc. Natl. Acad. Sci. USA.* **1999**, *96*, 14789.
111. Clarke, T. A.; Yousafzai, F. K.; Eady, R. R. *Biochemistry* **1999**, *38*, 9906.
112. Marquis, R. E. *Canadian Journal of Microbiology* **1995**, *41*, 955.
113. Gedanken, A. *Ultrasonics Sonochemistry* **2004**, *11*, 47. תווך
114. Suslick, K.S.; Choe, S. B.; Cichowlas, A.A.; Grinstaff, M. W. *Nature* **1991**, *353*, 414.
115. Hiller, R.; Putterman, S.J.; Barber, B.P. *Phys. Rev. Lett.* **1992**, *69*, 1182.
116. Suslick, K.S.; Hammerton, D.A.; Cline, R.E. *J. Am. Chem. Soc.* **1986**, *108*, 5641.
117. K.S. Suslick, D.A. Hammerton, R.E. Cline, J. Am. Chem. Soc. *108* (1986) 5641. תווך כמור 113
118. Ghows, N.; Entezari, M. H. *Ultrasonics Sonochemistry* **2010**, *17*, 878.
119. Cao, X.; Koltypin, Y.; Prozorov, R.; Katabya, G.; Gedanken, A. *J. Mater. Chem.* **1997**, *7*, 2447.
120. Kandjani, A. E.; Tabrizi, M. F.; Pourabbas, B. *Materials Research Bulletin* **2008**, *43*, 645.
121. Kumar, R. V.; Diamant, Y.; Gedanken, A. *Chem. Mater.* **2000**, *12*, 2301.
122. Margulis, M.A. *Russ. J. of Phys. Chem.* **1997**, *71*, 170.
123. Suslick, K. S.; Cline, Jr.; R. E.; Hammerton, D. A. *IEEE Ultrasonics Symp. Proc.* **1985**, *4*, 1116.
124. Flint, E. B.; Suslick, K. S. *J. Amer. Chem. Soc.* **1989**, *111*, 6987.

125. Suslick, K. S. *Scientific American* **1989**, 260, 80.
126. Gedanken, A. *Ultrasonics Sonochemistry* **2004**, 11, 47.
127. Adewuyi, Y. *Industrial & Engineering Chemistry Research* **2001**, 40, 4681.
128. Small- eyal
129. Shemesh, M.; Tam, A.; Aharoni, R.; Steinberg, D. *BMC Microbiol.* **2010**, 10, 51.
130. Lipovsky, A.; Tzitrinovich, Z.; Friedmann, H.; Applerot, G.; Gedanken, A.; Lubart, R. *J. Phys. Chem. C* **2009**, 113, 15997.
131. Applerot, G.; Lipovsky, A.; Dror, R.; Perkas, N.; Nitzan, Y.; Lubart, R.; Gedanken, A. *Adv. Funct. Mater.* **2009**, 19, 842.
132. Moody, C. S.; Hassa, H. M. *Proc. Natl. Acad. Sci. USA.* **1982**, 79, 2855.
133. Hassan, M. Fridovich, I. *J. Biol. Chem.* **1979**, 254, 10846.
134. Applerot, G.; Lellouche, J.; Lipovsky, A.; Nitzan, Y.; Lubart, R.; Gedanken, A.; Banin, E. *small* **2012**, 8, 3326.
135. Hernández-Sierra, J. F.; Ruiz, F.; Cruz Pena, D. C.; Martínez Gutiérrez, F.; Martínez, A. E.; Guillén, A. P.; Tapia-Pérez, H.; Castanon, G. M. *Nanomed. Nanotechnol.* **2008**, 4, 237.
136. Queiroz, A. M.; Nelson-Filho, P.; Silva, L. A.; Assed, S.; Silva, R. A.; Ito, I. *Y. Braz. Dent. J.* **2009**, 20, 290.
137. Valentine, J. S.; Doucette, P. A.; Zittin Potter, S. *Annu Rev Biochem.* **2005**, 74, 563.
138. T.J.Berger, J.A.Spadaro, S.E.Chapin, R.O.Becker, Antimicrob. Agents Chemother. **9** (1976) 357.
139. M.J. Domek, M.W. LeChevallier, S.C. Cameron, G.A. McFeters, *Appl. Environ. Microbiol.* **48** (1984) 289.
140. Hunter, J.M. *Geo. Rev.* **1973**, 63, 170.
141. Kawai, K.; Narushima, T.; Kaneko, K.; Kawakami, H.; Matsumoto, M.; Hyono, A.; Nishihara, H.; Yonezawa, T. *Applied Surface Science* **2012**, 262, 76.
142. Domek, M. J.; LeChevallier, M. W.; McFeters, G. A. *Appl. Environ. Microbiol.* **1984**, 48, 289.
143. Brookes, S.J.; Shore, R. C.; Robinson, C.; Wood, S.R.; Kirkham, J. *Arch Oral Biol.* **2003**, 48, 25.
144. Oppermann, R. V.; Johansen, J. R. *Scand. J. Dent. Res.* **1980**, 88, 476.
145. Afseth, J.; Oppermann, R. V.; Rolla, G. *Acta Odontol. Scand.* **1980**, 38, 229.
146. Oppermann, R. V.; Rolla, G. Johansen, J. R.; Assev, S. *Scand. J. Dent. Res.* **1980**, 88, 389.
147. Afseth, J.; Amsbaugh, S. M.; Monell-Torrens, E.; Bowen, W. H.; Rolla, G. Brunelle, J.; Dahl, E. *Caries Res.* **1984**, 18, 434.
148. Radovanovic, Z.; Veljovic, D.; Jokic, B.; Dimitrijevic, S.; Bogdanovic, G. Koic, V.; Petrovic, R.; Janackovic, D. *J. Serb. Chem. Soc.* **2012**, 77, 1787.
149. Kim, Y. M.; Farrah, S.; Baney, R. H. *Electron. J. Biotechnol.* **2006**, 9, 176.
150. Neal, A. L. *Ecotoxicology* **2008**, 17, 362.
151. Lellouche, J.; Kahana, E.; Elias, S.; Gedanken, A.; Banin, E. *Biomaterials* **2009**, 30, 5969.
152. Applerot, G.; Lipovsky, A.; Dror, R.; Perkas, N.; Nitzan, Y.; Lubart, R, et al. Enhanced antibacterial activity of nanocrystalline ZnO due to increased ROS-mediated cell injury. *Advanced Functional Materials* 2009;19:842-852. **83** רפרנט

153. Applerot G, Lellouche J, Lipovsky A, Nitzan Y, Lubart R, Gedanken A, et al. Understanding the antibacterial mechanism of CuO nanoparticles: revealing the route of induced oxidative stress. *Small* 2012;8:3326-3337. **רפרנט 130**
154. Koo, J.; Burrows, L. L.; Howell, P. L. *Fems Microbiology Letters* **2012**, 328, 1.
155. Galloway, D. R. *Molecular Microbiology* **1991**, 5, 2315.
156. Thill, A.; Zeyons, O.; Spalla, O.; Chauvat, F.; Rose, J.; Auffan, M.; Flank, A. M. *Environmental Science and Technology* **2006**, 40, 6151.
157. Kang, S.; Pinault, M.; Pfefferle, L. D.; Elimelech, M. *Langmuir* **2007**, 23, 8670.
158. Li, Y.; Zhang, W.; Niu, J.; Chen, Y. *Acs Nano* **2012**, 6, 5164.
159. Catala, A. *Chem. Phys. Lipids* **2009**, 157, 1.
160. Thill, A.; Zeyons, O.; Spalla, O.; Chauvat, F.; Rose, J.; Auffan, M.; A. M. Flank, *Environ. Sci. Technol.* **2006**, 40, 6151. **רפרנט 152**
161. Lovric, J.; Cho, S. J.; Winnik, F. M.; Maysinger, D. *Chem. Biol.* **2005**, 12, 1227.
162. Kang, S.; Pinault, M.; Pfefferle, L. D.; Elimelech, M. *Langmuir* **2007**, 23, 8670.
163. Skerl, K. G.; Segal, E.; Sreevalsan, T.; Scheld, W. M. *Can. J. Microbiol.* **1984**, 30, 221.
164. Courtney, H. S.; Ofek, I.; Simpson, W. A.; Hasty, D. L.; Beachey, E. H. *Infect. Immun.* **1986**, 53, 454.
165. Verceliotti, G. M.; Lussenhop, D.; Peterson, R. K.; Furcht, L. T.; McCarthy, J. B. H.; Jacob, S.; Moldow, C. F. *J. Lab. Clin. Med.* **1984**, 103, 34.
166. Simpson, W. A.; Beachey, E. H. *Infect. Immun.* **1983**, 39, 275.
167. Marquis, R. E.; Clock, S. A.; Mota-Meira, M. *FEMS Microbiol. Rev.* **2003**, 26, 93.
168. Puckett, S. D.; Taylor, E.; Raimondo, T.; Webster, T. J. *Biomaterials* **2010**, 31, 706.
169. Seil, J. T.; Rubien, N. M.; Webster, T. J.; Tarquinio, K. M. *J. Biomed. Mater. Res. B Appl. Biomater.* **2011**, 98, 1.
170. Singh, A. J.; Vyas, V.; Patil, R.; Sharma, V.; Scopelliti, P. E.; Bongiorno, G.; Podestà, A.; Lenardi, C.; Gade, W. N.; Milani, P. *PLoS One* **2011**, 6, e25029.
171. Vacheethasane, K.; Temenoff, J. S.; Higashi, J. M.; Gary, A.; Anderson, J. M.; Bayston, R.; Marchant, R. E. *J. Biomed. Mater. Res.* **1998**, 42, 425.
172. Hogt, A. H.; Dankert, J.; Vries, J. A.; Feijen, J.; Gen, J. *Microbiol.* **1983**, 129, 2959.
173. Quirynen, M.; Marechal, M.; Busscher, H. J.; Weerkamp, A. H.; Arends, J.; Darius, P. L.; Van Steenberghe, D. *J. Dent. Res.* **1989**, 68, 796.
174. Arita, N. K.; Shinonaga, Y.; Nishino, M. *Dent. Mater. J.* **2006**, 25, 684.
175. Dankert, J.; Hogt, A. H.; Feijen, J. *CRC. Crit. Rev. Biocompat.* **1986**, 2, 219.

